AR-001-399

DEPARTMENT OF DEFENCE

DEFENCE SCIENCE AND TECHNOLOGY ORGANISATION

ELECTRONICS RESEARCH LABORATORY

TECHNICAL REPORT

ERL-0037-TR

THE FREQUENCY RESPONSE OF A PARTICULAR GIMBAL SYSTEM TO COHERENT ROTATION AND ACCELERATION EXCITATION

R.F. Dancer

S U M M A R Y

The general theoretical expression for the frequency response of a gimbal system to a joint rotation/acceleration driving force is derived. Theoretical estimates of physical system parameters are made for a particular gimbal system. Experimental verification of these theories is obtained by measurements of the rotationally excited response of the gimbal system.

POSTAL ADDRESS: Chief Superintendent, Electronics Research Laboratory, Box 2151, G.P.O., Adelaide, South Australia, 5001.

TABLE OF CONTENTS

LIST OF APPENDICES

LIST OF TABLES

LIST OF FIGURES

1. INTRODUCTION

During testing of a miniature land navigation aid, the Infantry Automatic Position Indicating System (known as IAPIS) certain problems arose which required closer investigation. The detailed nature of the problem was evaluated and is discussed in reference 1, whilst the current study was instituted to establish a thorough understanding of the mechanical characteristics of the gimbal system incorporated in the Mk IV version of IAPIS.

The Mk IV version of IAPIS incorporates a gimballed magnetometer platform in order to maintain the magnetometers at an average horizontal attitude. This action was taken to eliminate the large errors that would result from the long-term slippage of a strapdown system on a man's back.

The gimbal system, whilst eliminating slippage, does respond to the short-period rotational and translational excitation experienced on the operator's back whilst he is walking. For responses on the pitch axis the fundamental component of such excitation may be represented by a rotation of the case and a horizontal acceleration (both at the pace frequency) with a fixed phase displacement. To predict navigation errors incurred by this response one needs to have a means of predicting the response of the system to a generalized excitation. A limited study of the rotational characteristics of a walking man is reported in reference 2.

2. THEORY OF GIMBAL MOTION

2.1 The model system

The model system, illustrated below, consists of three concentric components; the internal sphere, the external spherical case and the gimbal ring. The space between the sphere and the case is filled with a fluid of known viscosity, and specific gravity such that both sphere and gimbal ring are floating at neutral buoyancy. The sphere is free to rotate in the gimbal ring (on the pitch axis) and the gimbal ring is free to rotate within the case (on the roll axis), all bearings are frictionless. The pitch and roll axes lie in the horizontal plane and intersect orthogonally at the geometric centre of the system. The centre of mass of the sphere is located a known distance below its point of suspension (which is also its centre of buoyancy). The centre of mass of the gimbal ring and its geometric centre are coincident. Electrical connections between the sphere and the case are represented mechanically as springs.

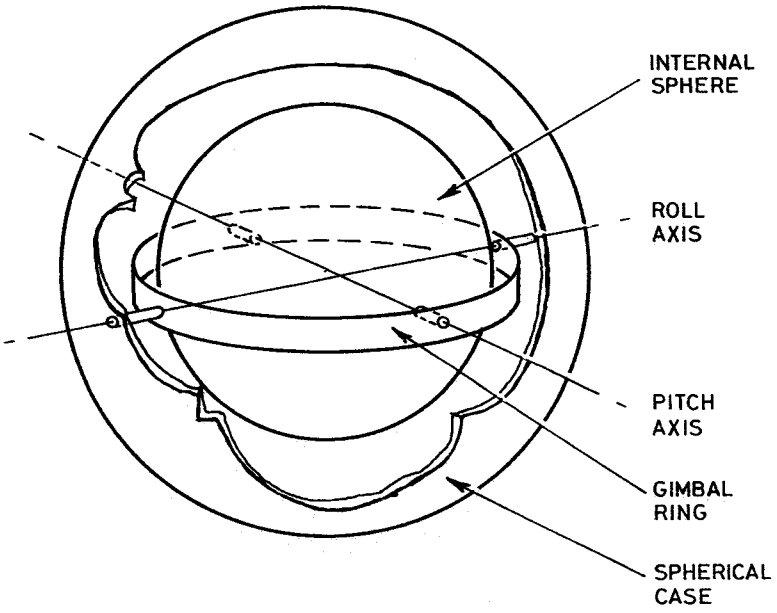

2.2 The equation of unforced motion

We need only consider rotations about one axis at a time since it can be shown that rotations about orthogonal axes are independent under certain conditions. These conditions hold true for the example system, the important consideration being that the axes of rotation are principal axes of the body that rotates. A schematic diagram representative of the single axis physical system is shown below.

We now define the various torques acting upon the central body when the case is held stationary.

The torque, τ_g, applied by gravity is expressed as:

$$\tau_g = - mg\, a_o \,\mathrm{Sin}\,\theta$$

where θ is the angular displacement of the central body, a_o is the offset of the centre of mass from the axis of rotation, g is the acceleration due to gravity and m is the mass of the central body. For small angles τ_g is given by:

$$\tau_g \cong - K_g\theta \qquad (1)$$

where K_g is termed the "gravity spring constant" and is given by:

$$K_g = mg\, a_o \qquad (2)$$

The torque, τ_s, applied by the springs is a function of the displacement θ. For small angles:

$$\tau_s \cong - K_s\theta \qquad (3)$$

Torque is exerted on the central body by viscous drag of the fluid, for non-turbulent flow this can be expressed as:

$$\tau_v = - L\dot{\theta} \qquad (4)$$

where $\dot{\theta}$ is the angular speed of the central body and L (termed the viscous torque coefficient) is some function of the interior geometry of the system and the coefficient of viscosity of the fluid.

If the moment of inertia of the system is I, then the equation of motion is obtained by summing the various torques in equations (1), (3) and (4) and putting this equal to the rate of change of angular momentum:

$$I\ddot{\theta} = \tau_g + \tau_s + \tau_v$$

or:

$$I\ddot{\theta} + L\dot{\theta} + (K_s+K_g)\theta = 0 \qquad (5)$$

The behaviour of the system when it is in a disturbed state ($\theta \neq 0$ or $\dot{\theta} \neq 0$) is obtained by solution of equation (5) only when no external "forces" are acting.

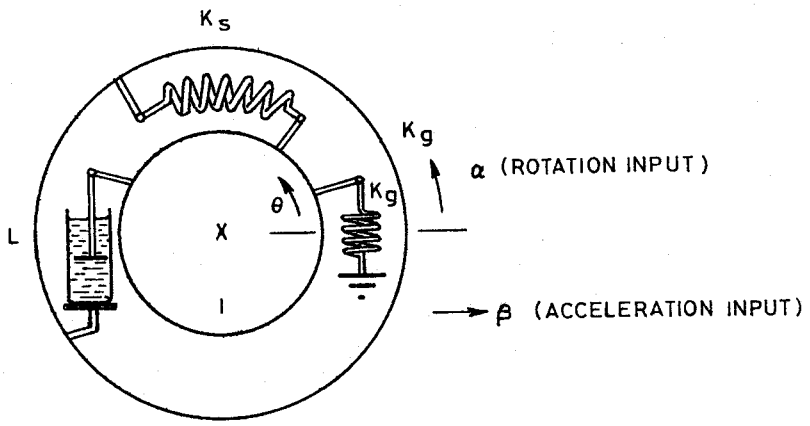

2.3 The equation of forced motion

The equation of motion when external "forces" are acting is obtained by substituting the driving torque for the zero on the right hand side of equation (5).

A driving torque is obtained by considering the torques acting upon the central body when it is held in an undisturbed state. Two possible sources of driving torque are considered; rotations of the case, and horizontal accelerations.

2.3.1 Rotational driving torque

A rotation of the case about the axis of interest by an angle α causes a rotation driving torque τ_a. This consists of some torque transmitted through the springs and some through the fluid, thus:

$$\tau_a = L\ddot{\alpha} + K_s\alpha \qquad (6)$$

2.3.2 Acceleration driving torque

A constant horizontal acceleration β, applied to the case exerts a force $-m\beta$ on the central body at a moment arm a_o. Hence the driving torque is given by:

$$\tau_b = m\beta a_o$$

or, rearranging: $$\tau_b = -K_g\gamma \tag{7}$$

where $\gamma = \beta/g$.

2.3.3 The complete equation of motion

The driving torque is obtained by summing equations (6) and (7). Thus the complete equation is:

$$I\ddot{\theta} + L\dot{\theta} + K\theta = L\dot{\alpha} + K_s\alpha - K_g\gamma \tag{8}$$

where $K = K_s + K_g$.

The output of the system, θ, for a given combination of inputs, α , γ, is obtained by solution of equation (8).

2.4 The frequency response

Taking the Laplace transform of equation (8) we obtain:

$$\Theta(s)\left[Is^2 + Ls + K\right] = A(s)\left[Ls + K_s\right] + \Gamma(s)\left[-K_g\right]$$

where

$$\Theta(s) = \mathcal{L}\{\theta(t)\}$$

$$A(s) = \mathcal{L}\{\alpha(t)\}$$

$$\Gamma(s) = \mathcal{L}\{\gamma(t)\}$$

This may be written as:

$$\Theta(s) = H_\alpha(s)\, A(s) + H_\gamma(s)\, \Gamma(s)$$

where

$$H_\alpha(s) = \frac{Ls + K_s}{Is^2 + Ls + K}$$

is the rotational transfer function, and

$$H_\gamma(s) = \frac{-K_g}{Is^2 + Ls + K}$$

is the acceleration transfer function.

The complex response of the system $G_\alpha(\omega)$ to a unit sinusoidal rotational input (the frequency response) is obtained as:

$$G_\alpha(\omega) = H_\alpha(j\omega) = \frac{K_s + jL\omega}{I(\omega_N^2 - \omega^2) + jL\omega} \tag{9}$$

and the frequency response to linear accelerations is:

$$G_\gamma(\omega) = H_\gamma(j\omega) = \frac{-K_g}{I(\omega_N^2 - \omega^2) + jL\omega} \tag{10}$$

where $$\omega_N^2 = \frac{K}{I} \qquad (11)$$

and $f_N = \omega_N/2\pi$ is termed the natural resonant frequency of the system.

Because the system is linear the output amplitude, R, when the system is excited by driving "forces" given by:

$$\alpha = \alpha_o e^{j\omega t}$$

$$\gamma = \gamma_o e^{j(\omega t+\delta)}$$

is:

$$R = \alpha_o G_\alpha(\omega) + \gamma_o e^{j\delta} G_\gamma(\omega) \qquad (12)$$

where δ is the phase lead of the acceleration relative to the rotation.

2.5 The zero frequency gain

In cases where the acceleration is zero the system response to a rotation at zero frequency is obtained from equations (9) and (11) as:

$$G_o = \frac{K_s}{K_s + K_g}$$

Hence for a gimbal system to be effective (in its primary function of eliminating long-term slippage of the sphere) K_s must be considerably less than K_g.

2.6 Example frequency responses

The absolute value and phase of the response R (from equation (12)) has been plotted in figures 1, 2 and 3 for a hypothetical system excited by rotation alone, acceleration alone, and a joint rotation-acceleration respectively. System parameters are I = 10.132, K_s = 40 and K_g = 360, which give f_N = 1.00 Hz and G_o = 0.1.

Figure 1 shows the case for which $\alpha_o = 1^o$ and $\gamma_o = 0$, figure 2 shows the case with $\alpha_o = 0$, $\gamma_o = 1^o$ and $\delta = \pi$ (for the damping coefficient L taking the values 10, 50 and 250 in both figures). These graphs show generally that larger damping coefficients yield larger values of response amplitude to rotation input and smaller responses to acceleration input.

The graphs plotted in figure 3 show the frequency response for the same system with damping coefficient fixed (L = 50) and $\alpha_o = \gamma_o = 1^o$ with input phase angle δ taking the values 0, $\pi/2$, π and $3\pi/2$.

It is seen that the response amplitude is strongly dependent upon the input phase angle at all frequencies.

3. MEASUREMENTS OF THE FREQUENCY RESPONSE OF THE EXAMPLE SYSTEM

The frequency responses of the example gimbal systems were determined by the measurement of their responses to a sinusoidal rotational excitation.

3.1 Measurement of the attitude of the internal sphere

As previously mentioned the internal sphere of the IAPIS gimbal system contains two magnetometers. These were utilized to enable measurement of its attitude, θ as explained below.

Suppose that a magnetometer is aligned at a heading of B (from magnetic north) and is inclined at a small angle θ to the horizontal, then the magnetic field along its own axis is given by:

$$H' \cong H'_H \text{ Cos } B + H'_V \theta$$

where H'_H and H'_V are, respectively, the horizontal and vertical components of the earth's field. If the inclination θ were varied from zero, the magnetometer output would vary from some fixed value, by an amount proportional to the amount of inclination. Thus the magnetometer output may be used as a measure of the inclination θ.

3.2 The rotation test equipment

The gimbal system under test was bolted to a rotating platform so that the axis of rotation was coincident with the gimbal axis. The platform was rocked sinusoidally through a crank arm, push rod, eccentric and gearbox by a variable speed electric motor. A photograph of this equipment is shown in figure 4.

Desired input frequencies were obtained by adjusting the motor speed (via a calibrated tachometer) and selection of the required gear ratio.

Actual platform inclinations, monitored electrically via a potentiometer attached to the platform axle, and internal magnetometer inclinations, monitored as described in Section 3.1, were recorded with timing pulses on a multi-channel chart recorder for later analysis.

3.3 Data analysis techniques

Pen records of input and output waveforms with timing were obtained at a set of frequencies between 0.02 Hz and 2.00 Hz (for an input amplitude of 5^o) for each gimbal axis. These records were analysed to yield a set of frequency, output amplitude and output phase lead ; $\{f_i, \theta_i, \psi_i\}$. The complex response amplitude Q was considered to take the form:

$$Q(\omega) = F.G_\alpha(\omega) \qquad (13)$$

where $G_\alpha(\omega)$ is defined in equation (9) and F, which has dimensions of length, is a constant for a particular set of data. Equation (13) gives the formulae for the expected values of amplitude and phase at angular frequency $= 2\,f$:

$$\left.\begin{aligned} \hat{\theta} &= |Q| = F \cdot \left(\frac{K_S^2 + L^2\omega^2}{(K - I\omega^2)^2 + L^2\omega^2} \right)^{1/2} \\ \hat{\psi} &= \text{Arg}(Q) = \arctan\left(\frac{I\omega(K_g - I\omega^2)}{K_S(K - I\omega^2) + L^2\omega^2} \right) \end{aligned}\right\} \qquad (14)$$

Simultaneous non-linear weighted regression was used to obtain the least-squares best fit of equations (14) to the set of data $\{f_i, \theta_i, \psi_i\}$, and the corresponding values of I, L and K_s.

These values depended upon the selection of an independent value for K_g. The selection procedure was changed according to the type of experimental information being gathered, as explained below.

3.3.1 Comparative measurements

The twelve sets of comparative measurements made on the system parameters of the six example gimbal units (each with 400 cs oil) were initially represented as two sets of six measurements of system parameters, both described by:

$$\{\tilde{I}_k \ , \ \tilde{L}_k \ , \ \tilde{K}_{s_k} \ , \ \bar{K}_g \} \qquad \text{for } k=1,\ldots,6$$

where $\bar{K}_g$ is the (constant) value estimated in Appendix III. However, it was decided that the value of L would be less likely to vary than would the value of K_g between the six units, since greater fabrication control could be maintained over external geometry (which is largely responsible for fixing L) than could be maintained over mass and its distribution within the sphere (which determines I and K_g). Consequently a scheme was devised in which each system's "measured" parameters were multiplied by a constant λ_k so as to bring all six viscous torque coefficients to a constant and maintain the mean average of the six values of K_g equal to $\bar{K}_g$. These constants are given by:

$$\lambda_k = \frac{1}{\tilde{L}_k}\left(\frac{1}{\frac{1}{6}\sum_{n=1}^{6}(1/\tilde{L}_n)}\right)$$

Then the new system parameter measurements are given by:

$$\{L_k, \ L, \ K_{s_k}, \ K_{g_k}\} = \{\lambda_k \tilde{I}_k, \ \lambda_k \tilde{L}_k, \lambda_k \tilde{K}_{s_k}, \lambda_k \bar{K}_g\}$$

The absolute accuracy of the results still depends upon the mean of the actual values of K_g for the six systems being equal to the estimated mean $\bar{K}_g$.

3.3.2 Measurements of one system with various oil viscosities

A series of measurements was made on the No.3 gimbal system after slight modifications with five different oil viscosities. In this case it was reasonable to assume that the values of K_g on the pitch and roll axes remained constant throughout. The two values used were obtained by subtracting from the final results for K_g of the No.3 system (from Section 3.3.1) the estimated change in K_g caused by the modification (as derived in Appendix III.2):

$$(K_g)_{pitch} = 849 - 259 = 590 \text{ dyne cm}$$

$$(K_g)_{roll} = 795 - 259 = 536 \text{ dyne cm}$$

4. SURVEY OF ALL EXAMPLE SYSTEMS

Six gimbal systems (numbered 1, 3, 4, 5, 6 and 7) were manufactured for use with IAPIS Mk IV (a photograph of one is shown in figure 5).

4.1 Comparative measurements of different systems

The rotational responses of each of the six gimbal systems has been measured (with 400 cs oil) on the pitch and roll axes. The results presented in Tables 1 and 2 list the measured values of I, L, K_s and K_g, the standard deviations of the residuals (errors between the fitted response functions and the data) in amplitude and phase; and the values of the natural frequency and the zero frequency gain.

Typical examples of the measured frequency response data and the best fit theoretical curves are given in figures 6 and 7 for the No.3 system on the pitch and roll axes respectively.

4.2 Measurements with different oil viscosities

The No.3 gimbal system, as modified (see Appendices I.7 and III.2) was tested with oil viscosities of 20, 50, 100, 250 and 400 cs. Tables 3 and 4 show the results (in the same form as Tables 1 and 2).

The frequency responses on the pitch and roll axes are given in figures 8 and 9 respectively. The measured moments of inertia and viscous torque coefficients are plotted vs. oil viscosity in figures 10 and 11 respectively.

5. DISCUSSION OF RESULTS

5.1 Sufficiency of theoretical treatment

5.1.1 Excellent agreement is observed over the stated range of frequency between the theoretical response functions derived in Section 2 and those measured experimentally. This agreement is exemplified by the results in figures 6 and 7. Further evidence of the agreement is given by the small residual standard errors given in Tables 1 and 2. The average deviation in amplitude being less than 1% of the maximum amplitude, and that of phase being equal to 1^{o}. Information given in Tables 3 and 4 shows that the fitting errors are generally larger for the smaller values of viscosity. This trend indicates that some theoretical assumption is starting to break down for thin oils (possibly that bearing friction is becoming a significant component at low frequency).

Because experimental verification of the theoretical treatment for the response to rotational excitation has been obtained, it may be inferred that the theory regarding the response to accelerations is also correct.

5.1.2 The values of the moments of inertia and viscous torque coefficients (for the 400 cs oil) calculated in Appendices I and II are tabulated below and compared with those values actually measured.

	Theory		Experimentally measured mean value
	Model 1	Model 2	
I_{pitch} (dyne cm s^2)	17.62	11.74	8.9
I_{roll} (dyne cm s^2)	27.60	34.92	25.4
L_{pitch} (dyne cm s)	625	870	776
L_{roll} (dyne cm s)	1181	2344	1422

As can be seen from these results, the model calculations were not very close to the experimental results, but the agreement is close enough to be useful for design purposes.

In the case of the series of measurements for various oils, the moments of inertia and viscous torque coefficients are plotted in figures 10 and 11. Again, there is reasonable agreement, for a range of viscosities, between the measured values plotted as data points and the theoretical lines.

5.2 Fabrication control

The measured values of I, K_s and K_g vary widely within the sample of six units as is seen in Tables 1 and 2. This variation is also reflected in the spread of values of natural frequency (from 1.31 Hz to 1.72 Hz and from 0.80 Hz to 0.96 Hz) and zero frequency gain (from 9% to 23% and from 11% to 15%).

NOTATION

a_o	offset of centre of mass from centre of suspension
d	thickness of fluid flow region
f	frequency
f_i	frequency of ith reading of system test output
f_N	natural resonant frequency
g	acceleration due to gravity
i	an index
j	the imaginary number $(-1)^{1/2}$
k	an index
l	length of a cylinder
l_1	thickness of a plane component
l_2	length of a cuboid
l_3	width of a cuboid
l_4	length of an elemental cuboid
m	a mass
n	an index
r	a radius
r_o, r_1	radii of a spherical shell of fluid
r_2, r_3	radii of a hollow right circular cylinder
r_4	internal radius of a ring solid
r_a	distance between centre of mass and axis of rotation of a body
r_e	external radius of ring solid
r_f	external radius of segments
r_i	internal radius of skin solid
r_k	average radius of spherical fluid flow
r_s	radius of element of fluid from axis of rotation
r_{sp}	radius of a spherical solid
s	variable in transform plane (of functions of time)
t	time
v	speed of fluid flow

w	angle of truncation of a circle
x, z	cartesian coordinates in calculation of effective moment of inertia of fluid
B	magnetic heading
F	a scale factor (units of length)
$G_\alpha(\omega)$	complex frequency response of gimbals to rotation input
G_o	zero frequency gain (value of $G^\alpha(0)$)
$G_\gamma(\ )$	complex frequency response of gimbals to acceleration input
$H_\alpha(s)$	transfer function of gimbals to rotation input
$H_\gamma(s)$	transfer function of gimbals to acceleration input
H'	resolved magnetic field strength
H'_H	horizontal magnetic field strength
H'_V	vertical magnetic field strength
I	a moment of inertia
$\tilde{I}_k$	kth initial measured moment of inertia
I_k	kth measured moment of inertia
I'_B	moment of inertia of a truncated spherical shell
I'_{CA}, I'_{CD}	moments of inertia of a cylinder on axis and diameter
I'_{CU}	moment of inertia of a cuboid
I'_F	effective moment of inertia of a truncated spherical shell with velocity gradient
I'_P	moment of inertia of a point mass
I'_{RA}, I'_{RD}	moments of inertia of a ring solid on axis and diameter
I'_S	moment of inertia of a spherical solid
I'_{SG}	moment of inertia of segments of a disc
$I_{i,p}$, $I_{i,r}$	moments of inertia of item i on pitch and roll axes
$I_{mod,p}$, $I_{mod,r}$	moments of inertia due to modification of unit 3
$I_{f1,p}$, $I_{f1,r}$	moments of inertia due to fluid flow (model 1)
$I_{f2,p}$, $I_{f2,r}$	moments of inertia due to fluid (model 2)
$J_n(w)$	(n=0,1,2,3,5) Definite integrals of cosine to the power n from 0 to w

K	total spring coefficient of model system
K_s	spring coefficients of electrical connections
$\tilde{K}_{s_k}$	kth initial measured value of K_s
K_{s_k}	kth measured value of K_s
K_g	gravitational spring coefficient of model system
K_{g_k}	kth measured value of K_g
$\overline{K}_g$	average (calculated) value of K_g
$(K_g)_{pitch}$, $(K_g)_{roll}$	estimated values of K_g for each axis of the number 3 gimbal system after modification
L	viscous torque coefficient
L'	relative viscous torque coefficient
$\tilde{L}_k$	initial measured viscous torque coefficient
L'_S	relative viscous torque coefficient of a truncated spherical flow
$L_{f1,p}$, $L_{f1,r}$	viscous torque coefficients of model 1 on pitch and roll axes
$L_{f2,p}$, $L_{f2,r}$	viscous torque coefficients of model 2
$L'_{f1,p}$, $L'_{f1,r}$	relative viscous torque coefficients of model 1
$L'_{f2,p}$, $L'_{f2,r}$	relative viscous torque coefficients of model 2
M_i	mass of item i
P	angular momentum
$Q(\omega)$	theoretical scaled rotation frequency response
R	total response to a coherent joint rotation/acceleration input
V_R	volume of ring solid
V_{SG}	volume of segments of a disc
X, Y, Z	cartesian coordinates of the model system
α	rotation driving input
α_o	amplitude of s nusoidal rotation driving input
β	linear acceleration
γ	acceleration driving input

γ_o	amplitude of effective sinusoidal rotation driving input (due to linear acceleration)
δ	phase between α and γ
η	viscosity
θ	angular displacement of central body
θ	theoretical amplitude of system test output
θ_i	amplitude of ith reading of system test output
θ_o	angular speed of fluid on inner spherical surface
θ_r	angular speed of fluid on spherical surface, radius r
θ'	co-latitude (in polar axes)
λ_k	constant scale factor for final processing of parameter measurements of kth unit
ρ	density of material (solid and liquid)
σ_G	standard deviation of residual errors in amplitude of system test output
σ_ψ	standard deviation of residual errors in phase of system test output
τ_a	rotation driving torque
τ_b	acceleration driving torque
τ_g	torque due to gravity
τ_s	torque due to springs
τ_v	viscous torque
φ	longitude (in polar axes)
$\hat{\psi}$	theoretical phase of system test output
ψ_i	phase of ith reading of system test output
ω	angular frequency
ω_N	natural resonant angular frequency
$A(s)$	Laplace transform of rotation driving input, $\alpha(t)$
$\Gamma(s)$	Laplace transform of acceleration driving input, $\alpha(t)$
Δ_A, Δ_B, Δ_C	contributions of fluid flow regions A, B and C
Δ_{CU}	contribution of cuboid
Δ_R	contribution of ring solid
Δ_S	contribution of spherical solid

Δ_{SG}	contribution of segments of disc
Δ_{Y}	contribution of cylinder
Δ_{A}	elemental surface area
ΔI_{r}	moment of inertia of elemental truncated spherical shell of radius r
ΔK_{g}	change in gravitational spring constant caused by modifications to unit 3
ΔP_{r}	angular momentum of elemental truncated spherical shell of radius r
ΔU	viscous drag on elemental surface area
Θ (s)	Laplace transform of system output, θ(t).

REFERENCES

No.	Author	Title
1	Dancer, R.F.	"Results of IAPIS Mk IV Development Trials (1975)". April 1976, WRE-TM-1556 (AP).
2	Dancer, R.F.	"Measurements of the Rotational Motion of a Walking Man". March 1976, WRE-TM-1398 (AP).

APPENDIX I

THEORETICAL ESTIMATES OF MOMENTS OF INERTIA

A model representation of the gimbal system with nineteen component parts is used for the computation of the pitch and roll moments of inertia. The total moment on each axis is obtained by summing the contributions of each component on that axis. A list of the various solid components and their contributions is given in Table 5. Planar projections of the model system are shown in figures 12, 13 and 14. The moment of inertia of any component depends upon its mass, shape, dimensions and orientation and position relative to the axis of interest.

I.1 Cylindrical components

All but five of the components have been considered to be uniform cylindrical solids. Their contributions to the moments of inertia are obtained by repeated application of three standard formulae. Given a uniform hollow right circular cylinder with radii r_2, r_3; length l and mass m; then its moment of inertia along its own axis is:

$$I'_{CA} = m(r_2^2 + r_3^2)/2 \qquad (I.1)$$

and its moment of inertia on a diameter through its centre is:

$$I'_{CD} = m((r_2^2 + r_3^2)/4 + l^2/12) \qquad (I.2)$$

If the centre of mass of any body is displaced by a distance r_a from the axis of rotation, then its moment of inertia is obtained as the sum of I'_P and that original moment about the axis that passes through its centre of mass parallel to the axis of rotation where:

$$I'_P = m r_a^2 \qquad (I.3)$$

The fourteen cylindrical components and their relevant parameters are listed in Table 6. The axial displacements are given by:

$$r_a = (X^2 + Z^2)^{1/2}$$

for the pitch axis, and:

$$r_a = (Y^2 + Z^2)^{1/2}$$

for the roll axis. This information is used in equations (I.1),(I.2) and (I.3) to calculate the contributions given in Table 5.

I.2 The skin component

This item is taken to be a uniform symmetrically truncated spherical shell. Its internal and external radii are $r_i = 0.950$ cm and $r_e = 1.397$ cm respectively. The two plane faces are parallel and circular, separated by a distance $l = 2.000$ cm. The pitch axis is coincident with the axis of symmetry and the roll axis lies in the plane of symmetry. The material is taken as having a density $\rho = 0.720$ g/cm^3.

For analytic reasons this component is broken down into three adjoining parts: a cylinder, a sphere and a ring with a spherical external surface and a cylindrical internal surface; this arrangement is shown in figure I.1. The contribution of the cylinder component to the skin moments of inertia on the pitch and roll axes are given by equations (I.1) and (I.2) respectively with m, r_2, r_3 and l taking the values:

$$\Delta_Y M_1 = m = \rho\pi \; r_4^2 \; l = 4.309 \text{ g}$$

$$r_4 = r_2 = (r_e^2 - (l/2)^2)^{1/2} = 0.976 \text{ cm}$$

$$r_3 = 0$$

$$l = 2.000 \text{ cm}$$

$$\Delta_Y I_{1,p} = I'_{CA} = 2.052 \text{ dyne cm s}^2$$

$$\Delta_Y I_{1,r} = I'_{CD} = 2.462 \text{ dyne cm s}^2$$

The contributions of the sphere component (to be subtracted from the skin totals) may be obtained from the moment of inertia of a general uniform sphere on any diameter mass m, radius r_{sp} as:

$$I'_S = 2/5 \; m \; r_{sp}^2 \qquad (I.4)$$

using the parameters:

$$r_{sp} = r_i = 0.950 \text{ cm}$$

and

$$-\Delta_S M_1 = m = \rho\pi \; 4/3 \; r_i^3 = 2.586 \text{ g}$$

then:

$$\Delta_S I_{1,p} = \Delta_S I_{1,r} = - I'_S = - 0.933 \text{ dyne cm s}^2$$

To evaluate the moments of inertia of a general solid ring (with a cylindrical interior, radius r_i, and spherical exterior, radius r_e) we divide it into elemental thin cylinders of radius r_2 and length l as shown below:

The moments of inertia of this thin cylinder on the axis of symmetry and on a diameter ΔI_A, ΔI_D are obtained by substituting Δm for m and $r_3 = r_2$ in equations (I.1) and (I.2) respectively:

$$\Delta I_A = I'_{CA} = \Delta m r_2^2$$

$$\Delta I_D = I'_{CD} = \Delta m(r_2^2/2 + l^2/12)$$

The mass Δm is given by:

$$\Delta m = \rho \Delta V$$

where the elemental volume is given by:

$$\Delta V = 2\pi r_2 \, l \, \Delta r_2$$

The total moments of inertia and volume of the ring are obtained by integrating ΔI_A, ΔI_D and ΔV over r_2 from r_4 to r_e:

$$I''_{RA} = \int_{r_4}^{r_e} \Delta I_A = 2\pi\rho \int_{r_4}^{r_e} (r_2^3 \, l) dr_2$$

$$I''_{RD} = \int_{r_4}^{r_e} \Delta I_D = 2\pi\rho \int_{r_4}^{r_e} (r_2^3 \, l/2 + r_2 \, l^3/12) dr_2$$

$$V_R = \int_{r_4}^{r_e} \Delta V = 2\pi \int_{r}^{r_e} (r_2 \, l) \, dr_2$$

noting that:

$$l = 2r_e \operatorname{Sin} \theta'$$

$$r_2 = r_e \operatorname{Cos} \theta' \qquad \text{so} \qquad dr_2 = - r_e \operatorname{Sin} \theta' \, d\theta'$$

$$\text{putting} \qquad w = \arccos (r_4/r_e)$$

and changing the variable of integration from r_2 to θ':

$$I'_{RA} = 4\pi\rho r_e^5 \int_0^w (\cos^3\theta' \ \sin^2\theta')d\theta' = 4\pi\rho r_e^5 (J_3(w) - J_5(w))$$

$$I''_{RD} = 4\pi\rho r_e^5 \int_0^w \left(\frac{\cos^3\theta' \ \sin^2\theta'}{2} + \frac{\cos\theta' \ \sin^4\theta'}{3}\right) d\theta'$$

$$= 4\pi\rho r_e^5 \left(\frac{1}{3}J_1(w) - \frac{1}{6}J_3(w) - \frac{1}{6}J_5(w)\right)$$

$$V_R = 4\pi r_e^3 \int_0^w (\cos\theta' \ \sin^2\theta')d\theta'$$

$$= 4\pi r_e^3 \ (J_1(w) - J_3(w))$$

Putting total mass $m = \rho \ V_R$, then:

$$I'_{RA} = m r_e^2 \left(\frac{J_3(w) - J_5(w)}{J_1(w) - J_3(w)}\right) \qquad (I.5)$$

$$I_{RD} = m r_e^2 \left(\frac{\frac{1}{3}J_1(w) - \frac{1}{6}J_3(w) - \frac{1}{6}J_5(w)}{J_1(w) - J_3(w)}\right) \qquad (I.6)$$

and

$$m = \rho \ 4\pi r_e^3 \ (J_1(w) - J_3(w)) \qquad (I.7)$$

where the functions $J_n(w)$ are defined by:

$$J_n(w) = \int_0^w \cos^n(\theta')d\theta'$$

It can be shown that these integrals may be evaluated from the recursive formula:

$$J_n(w) = \frac{n-1}{n} J_{n-2}(w) + \frac{1}{n}\sin w \cos^{n-1} w$$

with starting points:

$$J_o(w) = w \quad , \text{ for even values of n,}$$

and

$$J_1(w) = \sin(w), \text{ for odd values of n.}$$

Using the parameters $r_4 = 0.976$ cm, $r_e = 1.397$ cm then w = 0.7973 rad and from equation (I.7) the mass is given as:

$$\Delta_R M_1 = m = 3.017 \text{ g}$$

Equations (I.5) and (I.6) give the pitch and roll moment of inertia contributions as:

$$\Delta_R I_{1,p} = I''_{RA} = 4.076 \text{ dyne cm s}^2$$

and

$$\Delta_R I_{1,r} = I'_{RD} = 2.641 \text{ dyne cm s}^2$$

The whole skin component has mass given by:

$$M_1 = \Delta_Y M_1 + \Delta_S M_1 + \Delta_R M_1$$

$$= 4.74 \text{ g}$$

and moments of inertia:

$$I_{1,p} = \Delta_Y I_{1,p} + \Delta_S I_{1,p} + \Delta_R I_{1,p}$$

$$= 5.195 \text{ dyne cm s}^2$$

and

$$I_{1,r} = \Delta_Y I_{1,r} + \Delta_S I_{1,r} + \Delta_R I_{1,r}$$

$$= 4.170 \text{ dyne cm s}^2$$

I.3 The base plate

The base plate is assumed to be a uniform symmetrically truncated disc, $l_1 = 0.16$ cm thick, with radius $r_f = 1.350$ and, made from material with density $\rho = 1.96$ g/cm^3. The truncated faces are equal plane parallel rectangles separated by a distance $l_2 = 1.96$ cm and aligned so that the pitch axis passes through their centres. The roll axis is at right angles to this and is coincident with a diameter of the disc.

The pitch axis moment is formed by adding the moments of the rectangular plate and the segments of the disc, as shown in figure I.2. The moment of inertia of a cuboid of mass m with edges of length l_1, l_2 and l_3 on an axis through the centre of mass parallel with edges of length l_2 is given by:

$$I'_{CU} = m(l_1^2/12 + l_3^2/12) \qquad \text{(I.8)}$$

But:

$$l_3 = ((2r_f)^2 - l_2^2)^{1/2} = 1.857 \text{ cm}$$

and:

$$\Delta_{CU} M_6 = m = \rho\, l_1\, l_2\, l_3 = 1.141 \text{ g}$$

Applying these values to the formula for I'_{CU} gives:

$$\Delta_{CU} I_{6,p} = 0.331 \text{ dyne cm s}^2$$

To evaluate the moment of inertia of general segments (with radius r_f, thickness l_1, separated by distance l_2) on the axis shown, it is divided into pairs of elemental cuboids of length l_4 at radii r_a.

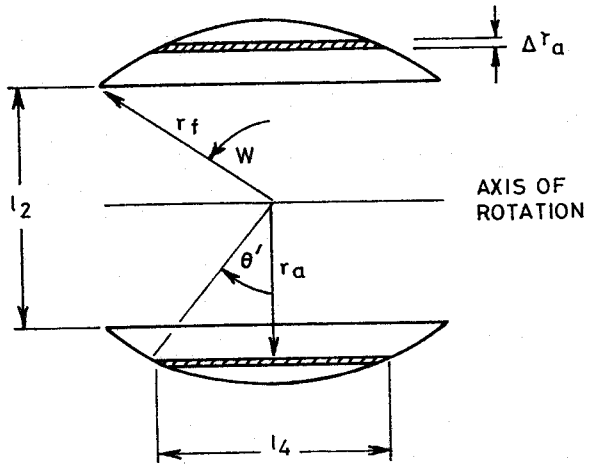

The moment of inertia of these two cuboids about the axis shown is obtained substituting Δm for m in equation (I.3) and $l_3 = \Delta r_a \to 0$ in equation (I.8) giving:

$$\Delta I = I'_{CU} + I'_P = \Delta m(r_a^2 + l_1^2/12)$$

The mass Δm is given by:

$$\Delta m = \rho \Delta V$$

where

$$\Delta V = 2 l_1 l_4 \Delta r_a$$

The total moment of inertia and volume are given by:

$$I'_{SG} = \int_{l_2/2}^{r_f} \Delta I = 2\rho l_1 \int_{l_2/2}^{r_f} l_4 (r_a^2 + l_1^2/12) dr_a$$

$$V_{SG} = \int_{l_2/2}^{r_f} \Delta V = 2 l_1 \int_{l_2/2}^{r_f} l_4 \, dr_a$$

but:

$$r_a = r_f \cos\theta'$$

$$dr_a = -r_f \sin\theta' \, d\theta'$$

and

$$l = 2 r_f \sin\theta'$$

Putting

$$w = \arccos(l_2 / 2r_f)$$

and changing the variable of integration from r_a to θ' :

$$I'_{SG} = 4\rho l_1 r_f^2 \int_0^w (\sin^2\theta' \left[r_f^2 \cos^2\theta' + l_1^2 / 12 \right]) d\theta'$$

$$= 4\rho l_1 r_f^2 \left(l_1^2 / 12 \left[J_o(w) - J_2(w) \right] + r_f^2 \left[J_2(w) - J_4(w) \right] \right)$$

and

$$V_{SG} = 4 l_1 r_f^2 \int_0^w (\sin^2\theta') d\theta'$$

$$= 4 l_1 r_f^2 \left[J_o(w) - J_2(w) \right]$$

Putting the total mass $m = \rho V_{SG}$ then:

$$I'_{SG} = m \left(l_1^2 / 12 + r_f^2 \left[\frac{J_2(w) - J_4(w)}{J_o(w) - J_2(w)} \right] \right) \qquad (I.9)$$

and

$$m = \rho \, 4 l_1 \, r_f^2 \left[J_o(w) - J_2(w) \right] \qquad (I.10)$$

The functions $J_n(w)$ are the same as defined in Section I.2. Using the values $l_1 = 0.16$ cm, $l_2 = 1.96$ cm and $r_f = 1.350$ cm then:

$$w = 0.812 \text{ rad}$$

$$\Delta_{SG} M_6 = m = 0.358 \text{ g}$$

and

$$\Delta_{SG} I_{6,p} = I'_{SG} = 0.438 \text{ dyne cm s}^2$$

The total mass and pitch axis moment of inertia contributions of this item are:

$$M_6 = \Delta_{CU} M_6 + \Delta_{SG} M_6$$

$$= 1.499 \text{ g}$$

and $$I_{6,p} = \Delta_{CU} I_{6,p} + \Delta_{SG} I_{6,p}$$

$$= 0.768 \text{ dyne cm s}^2$$

The roll axis moment is constructed by subtracting the moment of the missing segments from the moment of the disc (cylinder) as shown in figure I.2.

The mass of the disc is given by:

$$\Delta_Y M_6 = m = \rho\pi . r_f^2 l_1 = 1.7955 \text{ g}$$

Using this value of m and $r_1 = r_f = 1.35$ cm, $r_2 = 0$, $l = l_1 = 0.16$ cm in equation (I.2) we obtain:

$$\Delta_Y I_{6,r} = I'_{CD} = 0.8219 \text{ dyne cm s}^2$$

Equations (I.9) and (I.10) with:

$$w = \arccos (l_2/2r_f) = 0.758 \text{ rad}$$

give:

$$-\Delta_{SG} M_6 = m = 0.2962 \text{ g}$$

and $$\Delta_{SG} I_{6,r} = - I'_{SG} = - 0.4058 \text{ dyne cm s}^2$$

Thus $$I_{6,r} = \Delta_Y I_{6,r} + \Delta_{SG} I_{6,r}$$

$$= 0.416 \text{ dyne cm s}^2$$

and as a check on the calculations for the pitch axis

$$M_6 = \Delta_Y M_6 + \Delta_{SG} M_6 = 1.499 \text{ g}$$

is the same as before.

I.4 The internal sphere

The space inside the sphere, not occupied by other components is taken to be a uniform sphere of radius $r_{sp} = 0.95$ cm of material with density $= 0.111 \text{ g/cm}^3$. The mass is

$$M_{17} = m = \rho\pi . 4/3 \, r_{sp}^3 = 0.400 \text{ g}$$

and using equation (I.4) the moments of inertia are:

$$I_{17,p} = I_{17,r} = I'_S = 0.144 \text{ dyne cm s}^2$$

I.5 The gimbal ring

The gimbal ring (which only rotates on the roll axis) is considered as a uniform solid ring with a spherical exterior (r_e = 1.750 cm), cylindrical interior (r_2 = 1.475 cm) and two plane parallel ring faces separated by l = 1.640 cm. For analytic reasons it is divided into two adjoining solids as seen in figure I.3; a uniform hollow cylinder with external radius r_3 = 1.546 cm, and a ring solid as described in Section I.2. The density of the material is ρ = 1.43 g/cm^3.

The moment of inertia of the cylinder section is obtained by using equation (I.2) with:

$$\Delta_Y M_{18} = m = \rho\pi (r_1^2 - r_2^2) l = 1.580 \text{ g}$$

giving: $$\Delta_Y I_{18,r} = I'_{CD} = 2.158 \text{ dyne cm s}^2$$

The mass and moment of inertia of the ring solid are obtained from equations (I.6) and (I.7) with:

$$w = 0.4877 \text{ rad, and } r_4 = r_3 = 1.546 \text{ cm}$$

which give: $$\Delta_R M_{18} = m = 3.303 \text{ g}$$

and: $$\Delta_R I_{18,r} = I'_{RD} = 4.836 \text{ dyne cm s}^2$$

The total mass and moments of inertia of the gimbal ring are:

$$M_{18} = \Delta_Y M_{18} + \Delta_R M_{18}$$

$$= 4.883 \text{ g}$$

$$I_{18,p} = 0 \text{ dyne cm s}^2$$

$$I_{18,r} = \Delta_Y I_{18,r} + \Delta_R I_{18,r}$$

$$= 6.994 \text{ dyne cm s}^2$$

I.6 The fluid

The moment of inertia of the fluid can in principle be calculated for a particular flow pattern but this is complicated by the fact that velocity shears are present and that the flow pattern changes with viscosity. Two general cases are examined to determine the moments of inertia of partial spherical shells of fluid, firstly with no velocity gradient (i.e. the fluid moving as a solid body) and secondly with a constant velocity gradient across the gap.

The geometry of this problem is indicated below:

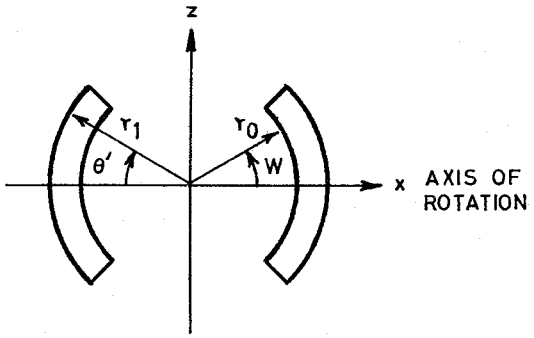

The moment of inertia of the thin spherical shell (truncated as shown) at radius r is given by the integral:

$$\Delta I_r = \int_{\theta' = -w}^{w} \int_{\varphi=0}^{2\pi} r_S^2 \; dm$$

where r_S is the distance between the element of mass dm in the shell and the axis of rotation but

$$r_S^2 = r^2 - x^2$$

$$= r^2 - r^2 \cos^2\theta' \; \cos^2\varphi$$

and

$$dm = \rho \, dV = \rho \Delta r . dA$$

but

$$dA = (r \cos\theta' \; d\varphi)(r d\theta')$$

$$= r^2 \cos\theta' \; d\theta' d\varphi$$

hence

$$\Delta I_r = 2\rho\Delta r \int_0^w \int_0^{2\pi} r^2 (1 - \cos^2\theta' \; \cos^2\varphi) \; r^2 \cos\theta' \; d\varphi \; d\theta''$$

$$= 2\pi\rho r^4 \Delta r \int_0^w (2\cos\theta' - \cos^3\theta') \, d\theta'$$

$$= 2\pi\rho r^4 \Delta r \left[2 J_1(w) - J_3(w) \right] \qquad \text{(I.11)}$$

If the fluid within the region shown is moving as one body then its moment of inertia is obtained by integrating ΔI_r over the limits of radius from r_o to r_1

$$I'_B = \int_{r_o}^{r_1} \Delta I_r = 2\pi\rho \left[2 J_1(w) - J_3(w) \right] \int_{r_o}^{r_1} r^4 \, dr$$

$$= 2\pi\rho \left[2 J_1(w) - J_3(w) \right] \left\{ \frac{r_1^5 - r_o^5}{5} \right\} \qquad (I.12)$$

In the second case we suppose that the fluid on any spherical shell has a constant angular speed $\dot{\theta}_r$ for a given speed $\dot{\theta}_o$ at $r = r_o$ and zero at $r = r_1$. In this case the angular momentum stored in a thin shell of fluid is:

$$\Delta P_r = \dot{\theta}_r \Delta I_r$$

Assuming that the angular speed is given by:

$$\dot{\theta}_r = \left(\frac{r_1 - r}{r_1 - r_o} \right) \dot{\theta}_o$$

The total angular momentum is given by:

$$P = \int_r \Delta P = \dot{\theta}_o \int_r \left(\frac{r_1 - r}{r_1 - r_o} \right) \Delta I_r$$

The second integral has the same physical significance as a moment of inertia. We term this the effective moment of inertia of the fluid (with the specified velocity gradient), i.e.:

$$I'_F = \int_{r_o}^{r_1} \left(\frac{r_1 - r}{r_1 - r_o} \right) \Delta I_r$$

$$= \frac{2\pi\rho}{r_1 - r_o} \left[2 J_1(w) - J_3(w) \right] \int_{r_o}^{r_1} (r_1 r^4 - r^5) dr$$

$$= \frac{\pi\rho}{15} \cdot \left[2 J_1(w) - J_3(w) \right] \left\{ \frac{r_1^6 - r_o^6}{r_1 - r_o} - 6 r_o^5 \right\} \qquad (I.13)$$

Two crude models of fluid flow behaviour around the sphere and gimbal ring are taken by arbitrarily dividing the fluid into regions (as shown in figures I.4 and 15) within which fluid flow properties are considered constant. The fluid density has been taken as $\rho = 0.965$ g/cm^3. Remembering that the gimbal ring moves on the roll axis and is fixed on the pitch axis, the flow behaviours for model 1 are tabulated below.

Axis of rotation	Fluid region		
	A	B	C
Pitch	Stationary	Velocity gradient	Velocity gradient
Roll	Velocity gradient	Moving as one body	Velocity gradient

The contribution of region A on the pitch axis is zero:

$$\Delta_A I_{f1,p} = 0 \text{ dyne cm s}^2$$

The contribution of region B on the pitch axis is obtained from equation (I.13) with $r_o = 1.397$, $r_1 = 1.581$ and $w = 0.4877$ rad.

$$\Delta_B I_{f1,p} = I'_F = 1.276 \text{ dyne cm s}^2$$

The contribution of region C on the pitch and roll axes is obtained for $r_o = 1.397$ cm, $r_1 = 1.905$ cm and subtracting the value of I'_F from equation (I.13) with $w = 0.4877$ rad from its value with $w = \pi$ 2 rad:

$$\Delta_C I_{f1,p} = \Delta_C I_{f1,r} = 12.807 - 4.830 = 7.977 \text{ dyne cm s}^2$$

Region A contributes an amount to the moment on the roll axis obtained from equation (I.13) with $r_o = 1.750$ cm, $r_1 = 1.905$ cm and $w = 0.4877$ rad:

$$\Delta_A I_{f1,r} = I'_F = 2.496 \text{ dyne cm s}^2$$

Region B acts as if it were a solid body so its moment on the roll axis is given by equation (I.12) with $r_o = 1.397$ cm, $r_1 = 1.581$ cm and $w = 0.4877$ rad:

$$\Delta_B I_{f1,r} = I'_B = 2.779 \text{ dyne cm s}^2$$

The total moments on the pitch and roll axes are obtained by summing the contributions from regions A, B and C:

$$I_{f1,p} = \Delta_A I_{f1,p} + \Delta_B I_{f1,p} + \Delta_C I_{f1,p} = 9.253 \text{ dyne cm s}^2$$

$$I_{f1,r} = \Delta_A I_{f1,r} + \Delta_B I_{f1,r} + \Delta_C I_{f1,r} = 13.252 \text{ dyne cm s}^2$$

The aspects of fluid flow in model 2, tabulated below, are illustrated in figure I.4.

Axis of rotation	Fluid region		
	A	B	C
Pitch	Not moving	Velocity gradient	Not moving
Roll	Velocity gradient	Moving as one body	Moving as one body

The contributions of regions A and C to the moment of inertia on the pitch axis are zero:

$$\Delta_A I_{f2,p} = \Delta_C I_{f2,p} = 0 \text{ dyne cm s}^2$$

The contribution of region B on the pitch axis is obtained from equation (I.13) with $r_o = 1.397$ cm, $r_1 = 1.581$ cm and $w = \pi/2$; hence:

$$\Delta_B I_{f2,p} = I'_F = 3.382 \text{ dyne cm s}^2$$

and:

$$I_{f2,p} = \Delta_A I_{f2,p} + \Delta_B I_{f2,p} + \Delta_C I_{f2,p} = 3.382 \text{ dyne cm s}^2$$

The contribution of region A on the roll axis is obtained by substituting $r_o = 1.750$ cm, $r_1 = 1.905$ and $w = \pi/2$ in equation (I.13):

$$\Delta_A I_{f2,r} = I'_F = 6.618 \text{ dyne cm s}^2$$

The contribution of region B is given by equation (I.12) with $r_o = 1.397$ cm, $r_1 = 1.581$ cm and $w = \pi/2$:

$$\Delta_B I_{f2,r} = I'_B = 7.368 \text{ dyne cm s}^2$$

The contribution of region C is given by equation (I.12) with $r_o = 1.581$ cm, $r_1 = 1.750$ cm and $w = \pi/2$, then subtracting the value of equation (I.12) with $w' = 0.4877$:

$$\Delta_C I_{f2,r} = 10.567 - 3.985 = 6.582 \text{ dyne cm s}^2$$

The total fluid contribution to the roll axis moment of inertia according to the second model is:

$$I_{f2,r} = \Delta_A I_{f2,r} + \Delta_B I_{f2,r} + \Delta_C I_{f2,r} = 20.568 \text{ dyne cm s}^2$$

The overall results for the system with the 18 solid components and each of the model fluid contributions are given in Table 5. The contributions of the fluid for each model are summarized below.

Axis of rotation	Moment of inertia (dyne cm s^2)	
	Model 1	Model 2
Pitch	9.25	3.38
Roll	13.25	20.57

I.7 Changes in the No.3 system

The No.3 system was modified by the removal of the two central balance screws "D" and "G", the two holes being left open. The changes in the system's moments of inertia are assumed to be the same as the original contributions of these items.

$$I_{mod,p} = - 0.53 \text{ dyne cm } s^2$$

$$I_{mod,r} = - 0.14 \text{ dyne cm } s^2$$

I.8 Total moments of inertia

The sums of the contributions of the 18 solid components in the standard and modified systems and the sums plus the additional contributions of the fluid, according to model 1 and model 2, are tabulated below.

	I pitch (dyne cm s^2)	I roll (dyne cm s^2)
Standard : basic	8.37	14.35
model 1	17.62	27.60
model 2	11.74	34.92
Modified : basic	7.84	14.21
model 1	17.09	27.46
model 2	11.22	34.78

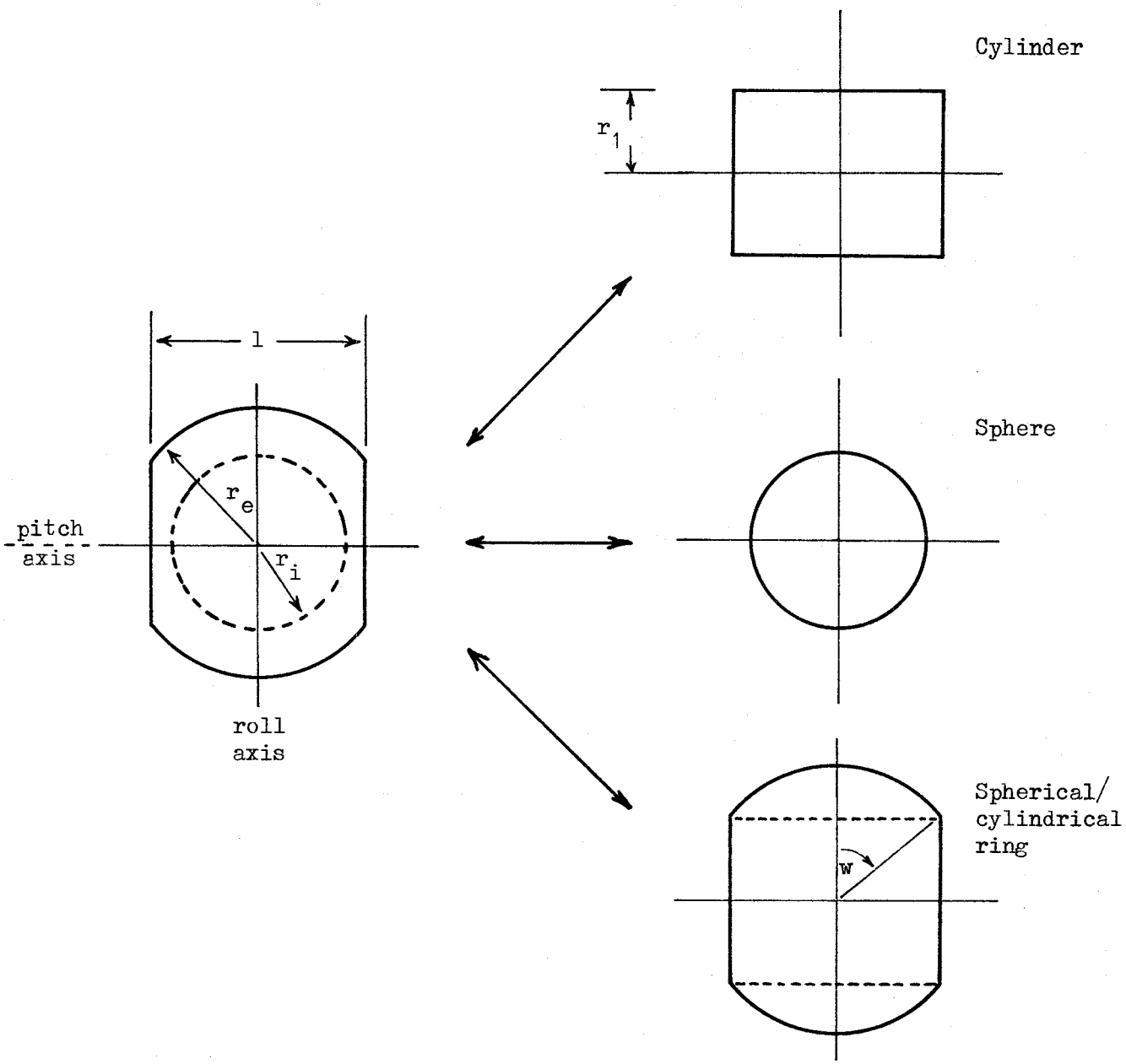

Figure I.1. Geometry for analysis of skin moments of inertia

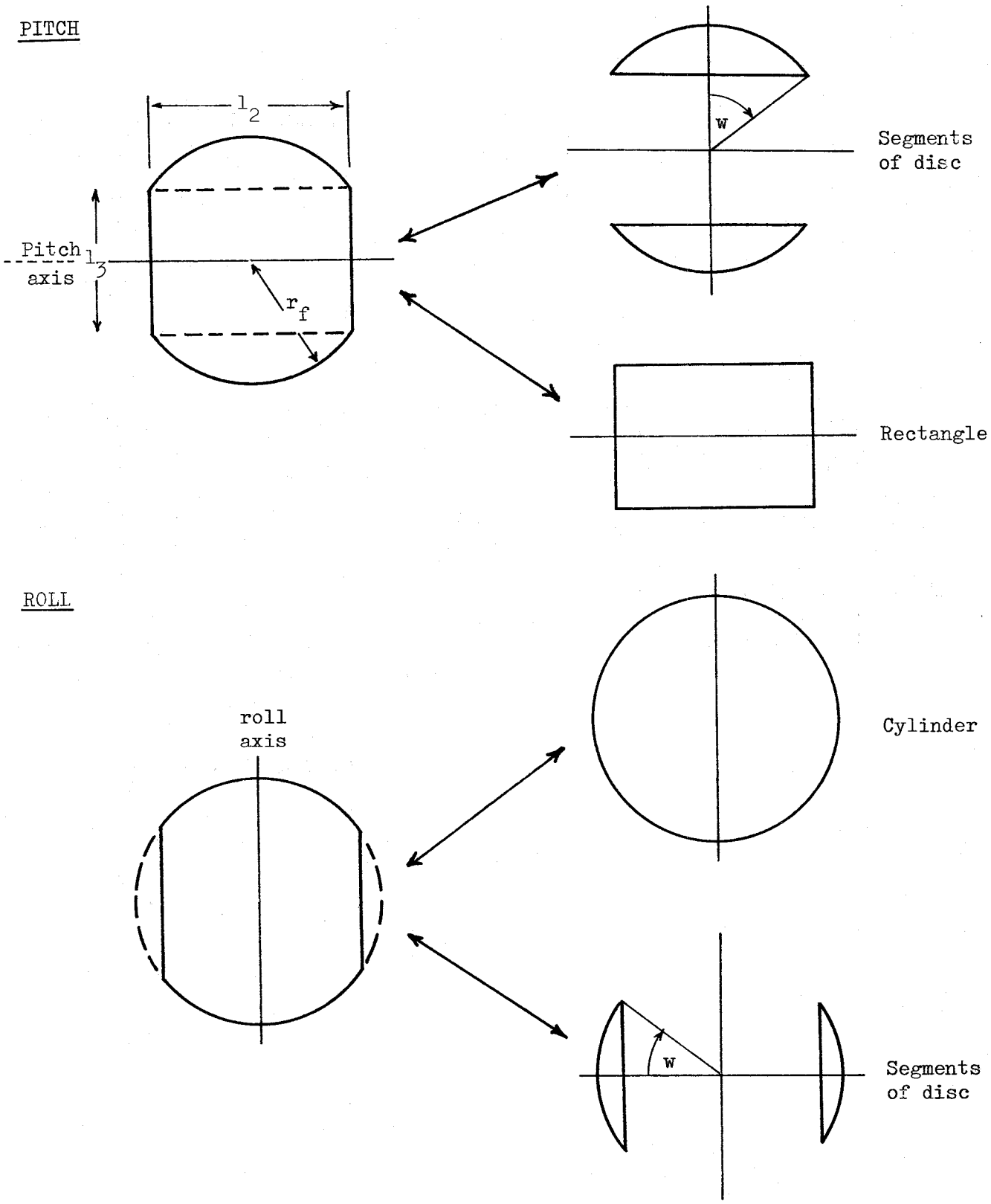

Figure I.2. Geometry for analysis of base plate moments of inertia

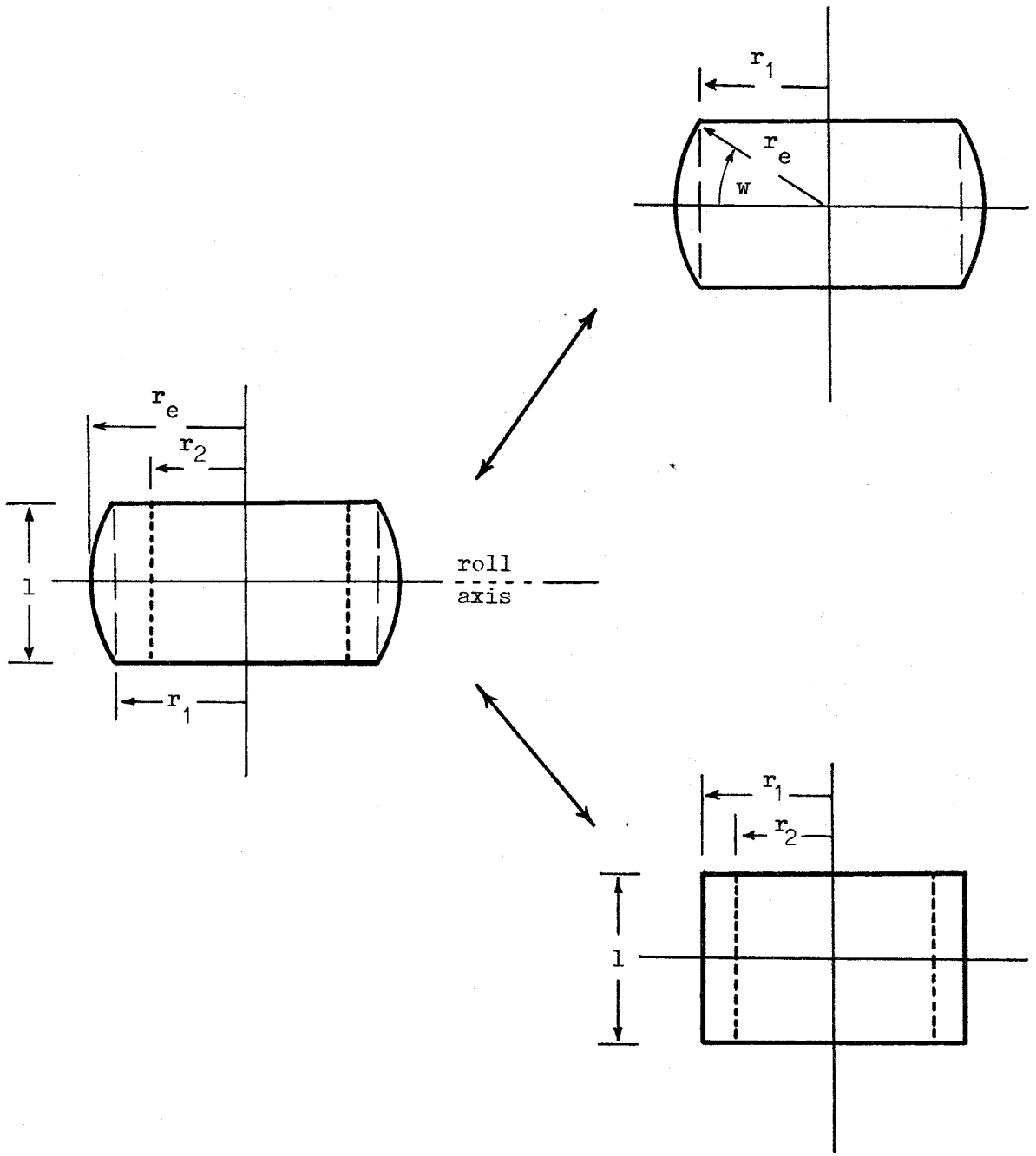

Figure I.3. Geometry for analysis of gimbal ring moment of inertia

Model 1

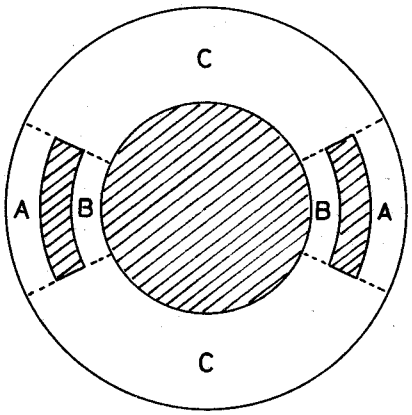

Model 2

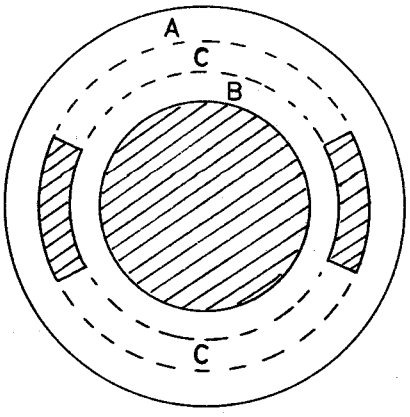

Figure I.4. Representation of fluid regions for calculation of contributions to moments of inertia and viscous torque coefficients

APPENDIX II

THEORETICAL CALCULATION OF VISCOUS TORQUE COEFFICIENTS

A full analysis of time-varying viscous flow of the damping fluid is not attempted. Instead, viscous effects for parallel surfaces are considered where the angular speed is constant.

The viscous force ΔU acting on an elemental area ΔA is given by:

$$\Delta U = \left(\frac{\eta v}{d}\right) \Delta A$$

where η is the coefficient of viscosity of the fluid, d is the separation of the surfaces and v is their relative speed. This force acts at right angles to the surface and is thus also at right angles to the axis of rotation at some distance r_s from that axis. The speed may thus be expressed as:

$$v = r_s \dot{\theta}$$

where $\dot{\theta}$ is the angular speed. The elemental applied torque $\Delta\tau$ is obtained as the product of the force and its moment arm:

$$\Delta\tau = r_s \Delta U = \eta/d \; r_s^2 \; \dot{\theta} \; \Delta A$$

The total torque due to viscous effects, τ_v, is obtained by integrating $\Delta\tau$ over the surface of interest, and if d is constant this is:

$$\tau_v = \left(\frac{\eta}{d} \oiint_{\text{SURFACE}} r_s^2 \; dA \right) \dot{\theta}$$

Hence the viscous torque coefficient is given by:

$$L = \left[\frac{1}{d} \oiint_{\text{SURFACE}} r_s^2 \; dA \right] \eta \qquad \text{(II.1)}$$

and we define L' by:

$$L' = L/\eta$$

The torque coefficients of the example system are defined by various combinations of spherical and truncated spherical component surfaces. Two differing models of fluid flow are assumed, as described in Appendix I.6, and illustrated in figure I.4 and figure 15.

The integral in equation (II.1) is evaluated for a general truncated spherical surface, radius r_k, truncated at colatitude $\theta' = w$ and rotating about the x axis:

$$r_s^2 = r_k^2 - r_k^2 \; \text{Cos}^2\theta' \; \text{Cos}^2\varphi$$

$$dA = (r_k \; \text{Cos} \; \theta' \; d\varphi)(r_k d\theta')$$

Thus

$$L'_S = 2\frac{r_k^4}{d}\int_0^w\int_0^{2\pi}(\cos\theta' - \cos^3\theta'\ \cos^2\varphi)\,d\varphi\,d\theta'$$

$$= \frac{2\pi r_k^4}{d}\int_0^w(2\cos\theta' - \cos^3\theta')\,d\theta'$$

Thus

$$L'_S = \frac{2\pi r_k^4}{d}\left[2J_4(w) - J_3(w)\right] \qquad \text{(II.2)}$$

The functions $J_n(w)$ are the same as described in Appendix I.2.

Using model 1, region A is stationary and so adds nothing to the torque coefficient. Region B contributes an amount on the pitch axis, given by equation (II.2) with d = 0.184 cm being the gap, and r_k = 1.4890 cm is taken to be the average radius, and w = 0.4877 rad:

$$\Delta_B L_{f1,p} = L'_S = 84.41 \text{ dyne cm s/poise}$$

The contributions of region C to both pitch and roll axes are obtained from equation (II.2) with d = 0.508, r_k = 1.651 and subtracting from its value with w = $\pi/2$ (the whole sphere) the value with w = 0.4877 rad (that part covered by the gimbal ring) giving:

$$\Delta_C L'_{f1,p} = \Delta_C L'_{f1,r} = L'_S = 76.32 \text{ dyne cm s/poise}$$

The total torque coefficient on the pitch axis is given as:

$$L_{f1,p} = \left[\Delta_B L'_{f1,p} + \Delta_C L'_{f1,p}\right]\eta$$

$$= 160.73\,\eta \text{ dyne cm s}$$

The contribution of region A on the roll axis is obtained from equation (II.2) with d = 0.155 cm, r_k = 1.8275 cm and w = 0.4877:

$$\Delta_A L'_{f1,r} = L'_S = 227.37 \text{ dyne cm s/poise}$$

The contribution of region B to viscous torque on the roll axis is zero since there is no velocity gradient. The total torque coefficient on the roll axis is thus given as:

$$L_{f1,r} = \left[\Delta_A L_{f1,r} + \Delta_C L_{f1,r}\right]\eta$$

$$= 303.69\,\eta \text{ dyne cm s}$$

Using model 2 the only contribution on the pitch axis is from region B. This is obtained from equation (II.2) with d = 0.184 cm, r_k = 1.4890 cm and w = $\pi/2$:

$$\Delta_B L'_{f2,p} = L'_S = 223.81 \text{ dyne cm s/poise}$$

Thus the pitch axis torque coefficient is:

$$L_{f2,p} = 223.81 \eta \text{ dyne cm s}$$

The only contribution, in model 2, to the torque coefficient on the roll axis comes from region A. Using equation (II.2) with d = 0.155 cm, r_k = 1.8275 cm and w = $\pi/2$ we obtain:

$$\Delta_A L'_{f2,r} = L'_S = 602.86 \text{ dyne cm s/poise}$$

The torque coefficient on the roll axis is:

$$L_{f2,r} = 602.86 \eta \text{ dyne cm s}$$

The results are summarised below

Axis of rotation	Viscous torque coefficient (dyne cm s)	
	Model 1	Model 2
Pitch	160.7 η	223.8 η
Roll	303.7 η	602.9 η

and plotted as straight lines in figure 11. The values of density and viscosity for oils used in the experiments are given in Table 7.

APPENDIX III

THEORETICAL ESTIMATES OF GRAVITATIONAL SPRING CONSTANT

The restoring torque per unit angular displacement (spring constant) due to gravity is given by:

$$K_g = m g a_o$$

where m is the mass of the inner sphere,

g is the acceleration due to gravity (981 cm s^{-2}), and

a_o is the offset of the centre of mass of the sphere below its centre of suspension.

Alternatively, it is equivalent to consider only the centres of mass and masses of those unbalanced components.

III.1 The standard system

The only items unbalanced are the balance adjustment screws, but in the calculations of Appendix I for the moments of inertia it has been assumed that the skin component and the six balance screws occupy the same space. This approximation may be improved here by subtracting from the mass of the balance screws, the mass of skin material excavated to form the screw holes.

For six holes each 0.7 cm deep, 0.125 cm radius the volume of missing material is 0.206 cm^3. Hence, taking the density as 0.72 g/cm^3 the missing mass is 0.148 g.

From Table 6 we take the mass of six balance screws as 1.56 g, and their overall centre of mass offset is a_o = 0.508 cm. This produces an effective mass of 1.41 g offset by 0.508 cm, giving:

$$K_g = 703 \text{ dyne cm}$$

It should be noted that the equivalent offset of the centre of mass of the sphere (of 10.65 g mass) is 0.067 cm (i.e. 0.026 inch).

III.2 Changes in the No.3 system

The two central balance screws were removed and their holes were left open. The effect of this is to reduce by 0.52 g, the mass offset by 0.508 cm. The change in K_g is thus given by:

$$\Delta K_g = - 259 \text{ dyne cm}$$

If the value of K_g for the No.3 system were exactly as calculated in Appendix III.1 then the offset of the sphere centre of mass would be 0.017 inch.

TABLE 1. COMPARATIVE MEASUREMENTS OF THE GIMBAL SYSTEMS

(PITCH AXIS: 400 cs OIL)

Gimbal system No.	Best fit parameters				Residual errors		Derived parameters	
	I	L	K_s	K_g	σ_G (%)	σ_φ (degrees)	f_N (Hz)	G_o (%)
1	9.3	776	80	551	0.9	1.0	1.31	13
3	8.3	776	127	849	1.1	2.0	1.72	13
4	8.0	776	184	613	0.4	1.1	1.58	23
5	8.7	776	92	704	0.6	1.3	1.52	12
6	9.6	776	78	756	0.7	0.6	1.49	9
7	9.7	776	93	745	0.9	0.7	1.48	11
Averages	8.9	776	109	703	0.8	1.1	1.51	14

TABLE 2. COMPARATIVE MEASUREMENTS OF THE GIMBAL SYSTEMS

(ROLL AXIS: 400 cs OIL)

Gimbal system No.	Best fit parameters				Residual errors		Derived parameters	
	I	L	K_s	K_g	σ_G (%)	σ_φ (degrees)	f_N (Hz)	G_o (%)
1	23.0	1422	84	496	1.2	0.9	0.80	15
3	26.1	1422	105	795	1.1	0.8	0.94	12
4	24.6	1422	87	659	1.1	1.2	0.88	12
5	22.3	1422	106	705	0.8	0.8	0.96	13
6	27.9	1422	126	746	1.1	0.8	0.89	15
7	28.4	1422	106	817	1.1	0.9	0.91	11
Averages	25.4	1422	102	703	1.1	0.9	0.90	13

TABLE 3. PITCH AXIS MEASUREMENTS OF THE MODIFIED NO. 3 GIMBAL SYSTEM VS OIL VISCOSITY

Fluid viscosity (cs)	Best fit parameters				Residual errors		Derived parameters	
	I	L	K_s	K_g	σ_G (%)	σ_φ (degrees)	f_N (Hz)	G_o (%)
20	7.2	48	84	590	3.3	1.6	1.54	12
50	6.6	105	64	590	0.9	2.3	1.58	10
100	7.7	186	64	590	1.2	1.4	1.47	10
250	8.3	512	67	590	0.5	1.0	1.41	10
400	9.5	801	69	590	0.9	1.2	1.32	11

TABLE 4. ROLL AXIS MEASUREMENTS OF THE MODIFIED NO. 3 GIMBAL SYSTEM VS OIL VISCOSITY

Fluid viscosity (cs)	Best fit parameters				Residual errors		Derived parameters	
	I	L	K_s	K_g	σ_G (%)	σ_φ (degrees)	f_N (Hz)	G_o (%)
20	22.6	97	109	536	1.6	6.0	0.85	17
50	21.7	188	97	536	1.7	3.4	0.86	15
100	22.6	344	134	536	0.8	1.6	0.87	20
250	26.3	969	101	536	0.9	0.6	0.78	16
400	28.1	1486	80	536	1.6	1.0	0.74	13

TABLE 5. COMPONENT MASSES AND THEIR MOMENTS OF INERTIA

($dyne.cm.s^2$)

Item number	Description	Mass	I_{ROLL}	I_{PITCH}
1	Skin	4.74	4.170	5.195
2	N Pickup Coil	0.46	0.046	0.173
3	E Pickup Coil	0.46	0.173	0.046
4	N Excitation Coils	0.15	0.011	0.095
5	E Excitation Coils	0.15	0.095	0.011
6	Base Plate	1.50	0.416	0.769
7	Disc A	0.38	0.446	0.160
8	Disc B	0.38	0.446	0.160
9	Bush A	0.24	0.414	0.014
10	Bush B	0.24	0.414	0.014
11	Screw C	0.26	0.111	0.264
12	Screw D	0.26	0.069	0.264
13	Screw E	0.26	0.111	0.264
14	Screw F	0.26	0.111	0.264
15	Screw G	0.26	0.069	0.264
16	Screw H	0.26	0.011	0.264
17	Foam Sphere	0.40	0.144	0.144
18	Gimbal Ring	4.88	6.994	0
	TOTALS: Basic Model	15.54	14.351	8.365
	: Model 1	-	27.60	17.62
	: Model 2	-	34.92	11.75

TABLE 6. PARAMETERS OF THE CYLINDRICAL COMPONENTS OF THE GIMBAL SYSTEM

Item number	Description	Axial alignment	Length (l)	External radius (r_2)	Internal radius (r_3)	Mass (m)	Position of the centre of mass		
							X	Y	Z
2	N Pickup Coil	Roll	1.88	0.16	0.09	0.46	0	0	0.254
3	E Pickup Coil	Pitch	1.88	0.16	0.09	0.46	0	0	-0.254
4	N Excitation Coils	Roll	2.60	0.09	0	0.15	0	0	0.254
5	E Excitation Coils	Pitch	2.60	0.09	0	0.15	0	0	-0.254
7	A Disc	Pitch	0.16	0.80	0.45	0.38	0	0.98	0
8	B Disc	Pitch	0.16	0.80	0.45	0.38	0	-0.98	0
9	A Bush	Pitch	0.28	0.30	0.15	0.24	0	1.30	0
10	B Bush	Pitch	0.28	0.30	0.15	0.24	0	-1.30	0
11	C Screw	Roll	0.601	0.125	0	0.26	0.85	0.40	-0.508
12	D Screw	Roll	0.601	0.125	0	0.26	0.85	0	-0.508
13	E Screw	Roll	0.601	0.125	0	0.26	0.85	-0.40	-0.508
14	F Screw	Roll	0.601	0.125	0	0.26	-0.85	0.40	-0.508
15	G Screw	Roll	0.601	0.125	0	0.26	-0.85	0	-0.508
16	H Screw	Roll	0.601	0.125	0	0.26	-0.85	-0.40	-0.508

TABLE 7. PHYSICAL PROPERTIES OF OILS

Kinematic viscosity (centi-stoke)	Density ($gm\ cm^{-3}$)	Viscosity (poise)
20	0.955	0.191
50	0.960	0.480
100	0.968	0.968
250	0.971	2.428
400	0.972	3.888

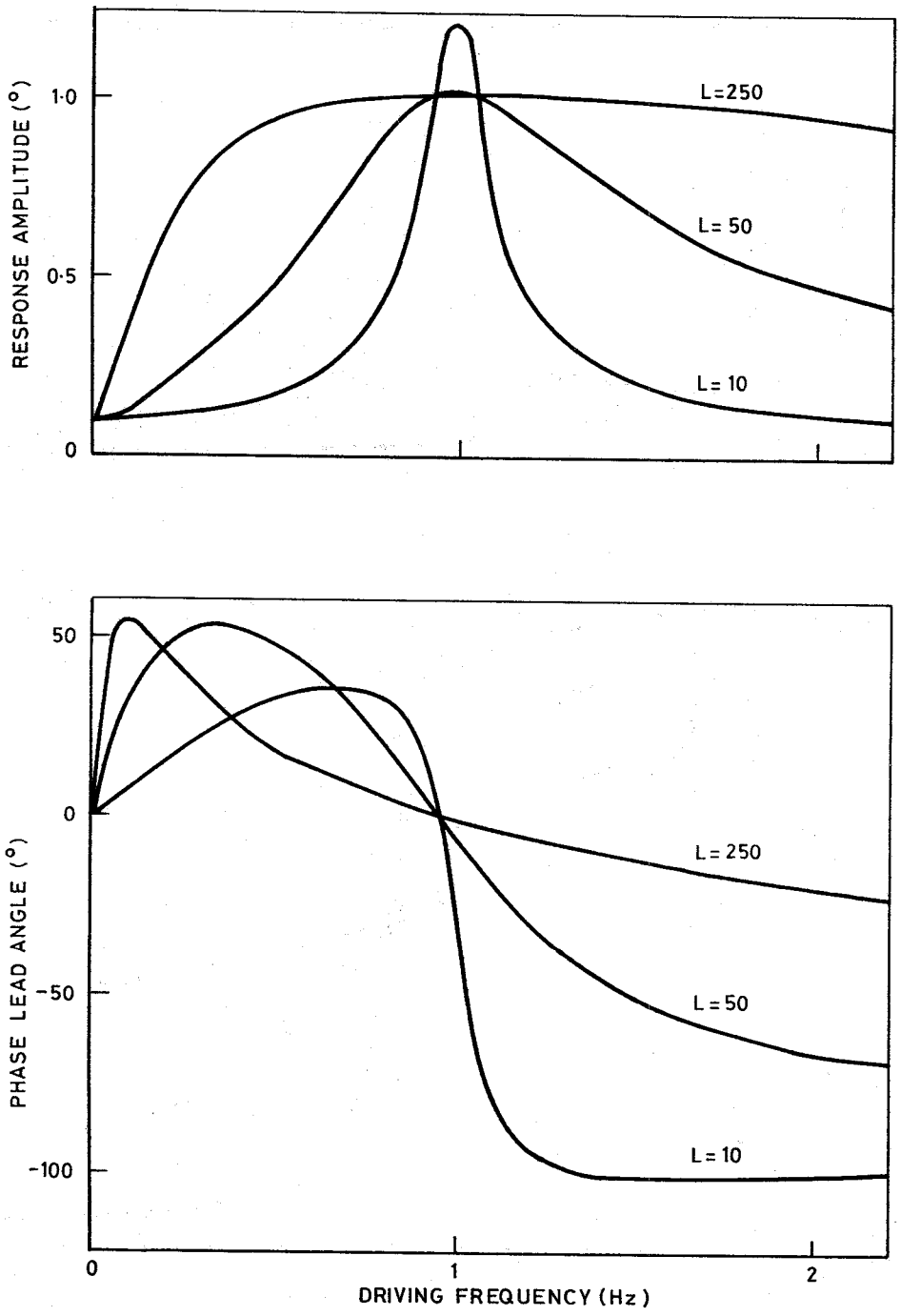

Figure 1. Examples of rotationally excited frequency responses

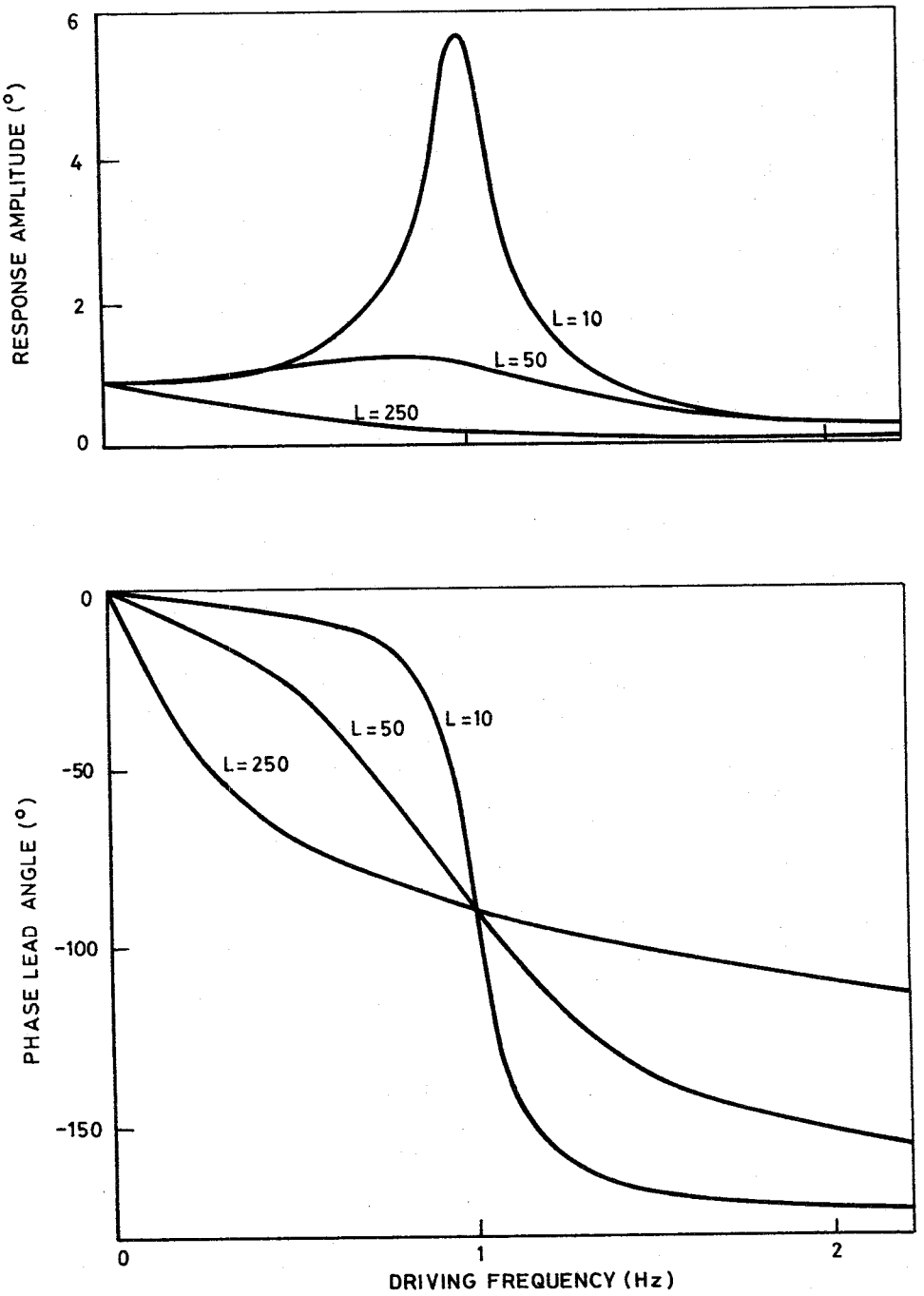

Figure 2. Examples of acceleration excited frequency responses

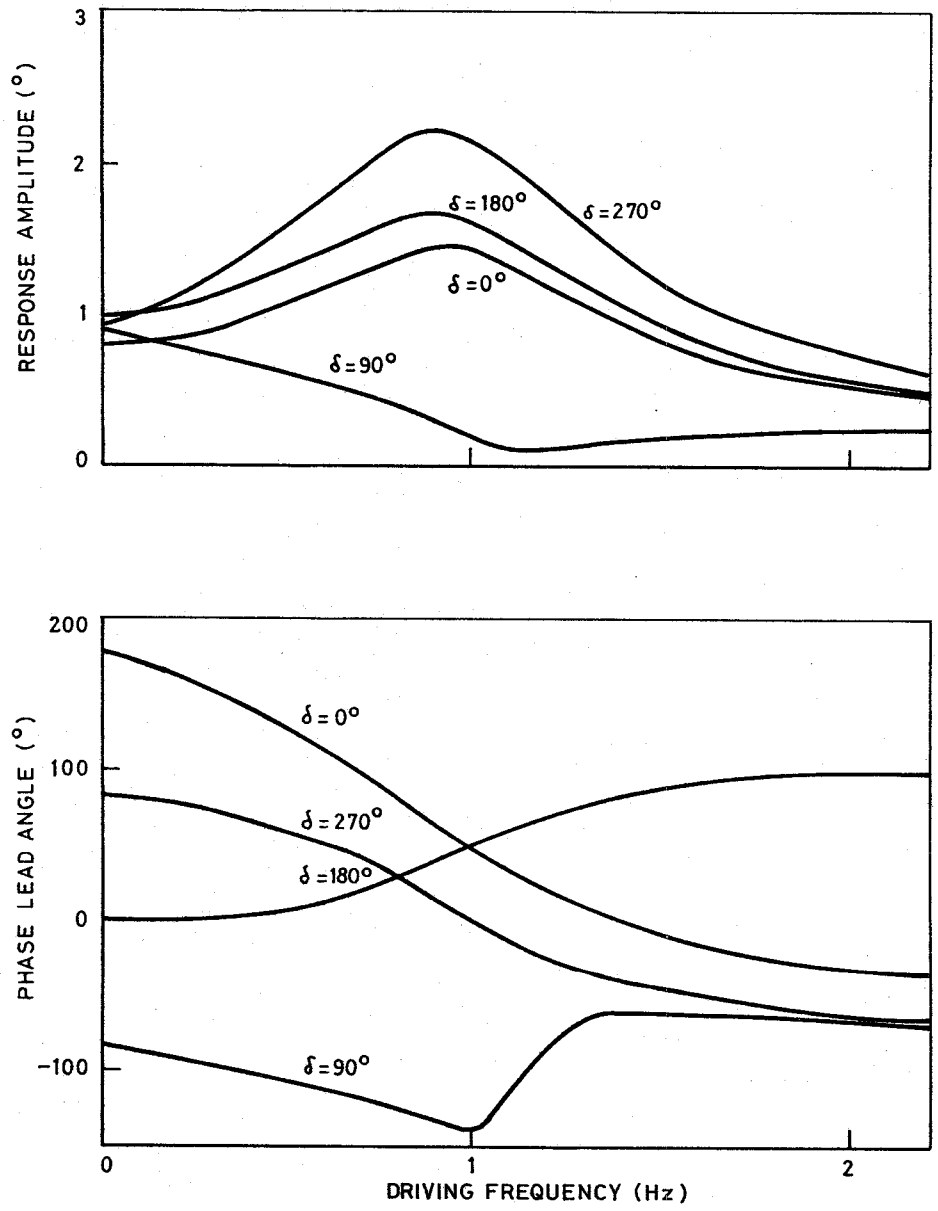

Figure 3. Examples of coherent rotation and acceleration excited frequency response

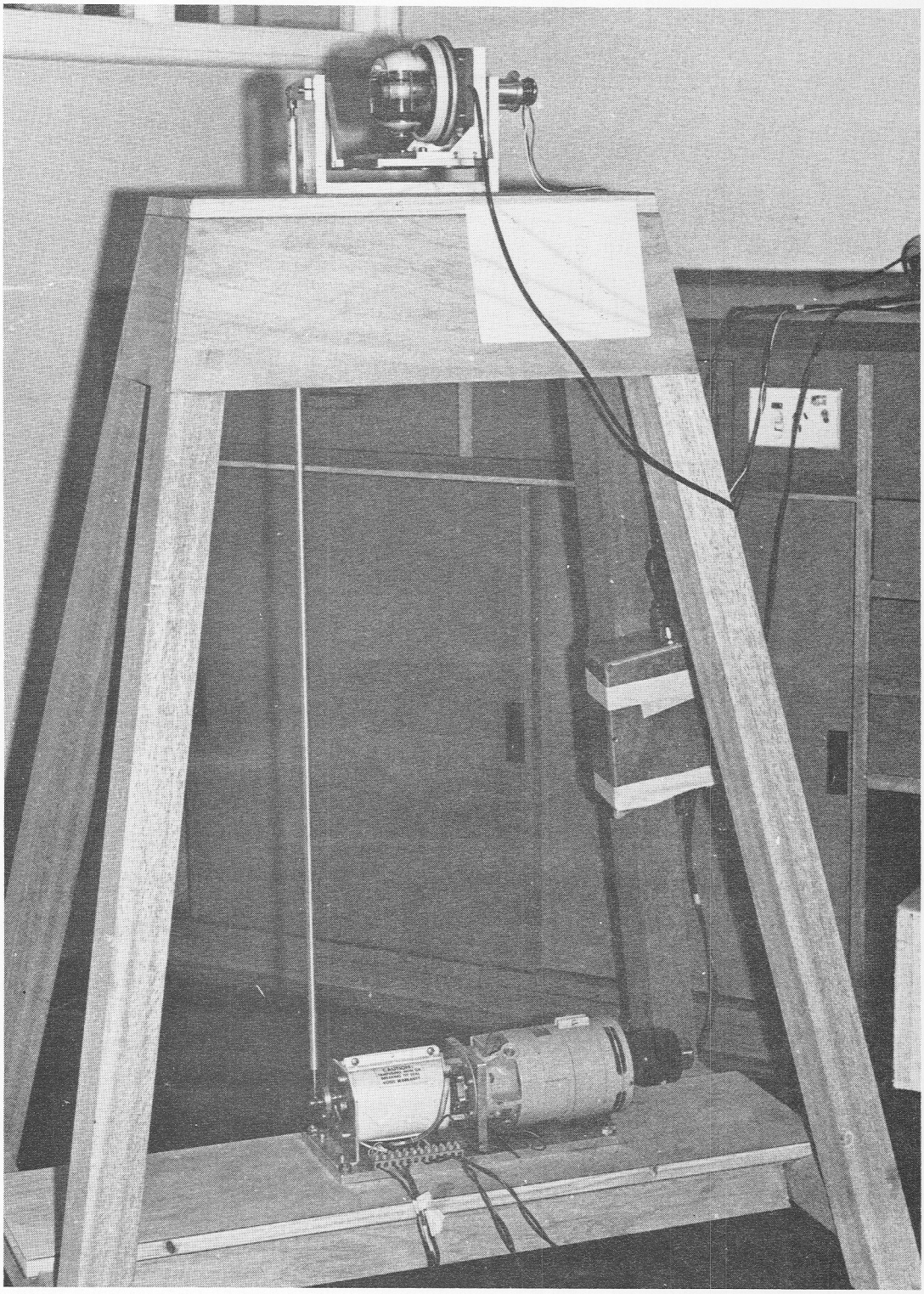

Figure 4. Photograph of the test rig

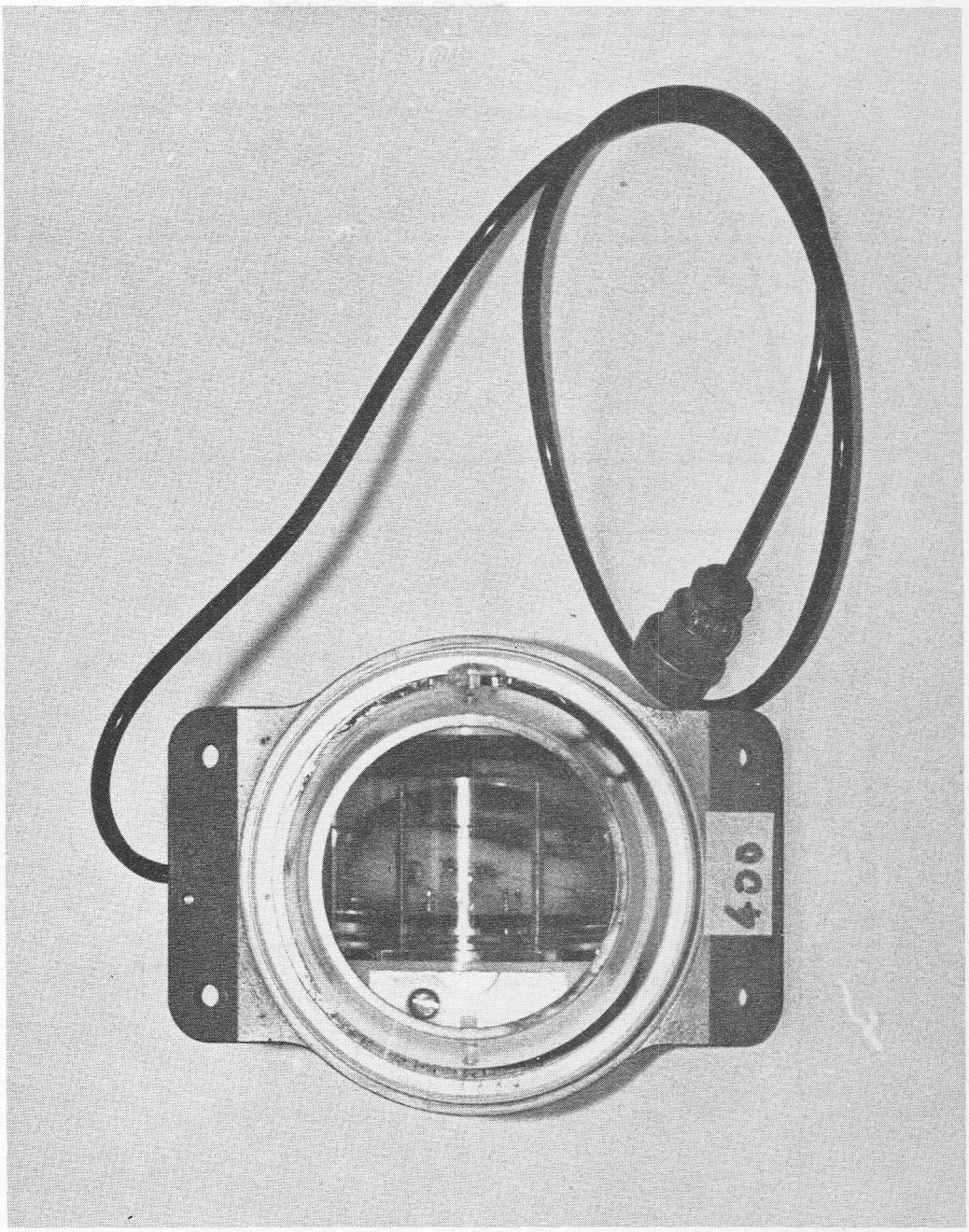

Figure 5. Photograph of the IAPIS gimbal system

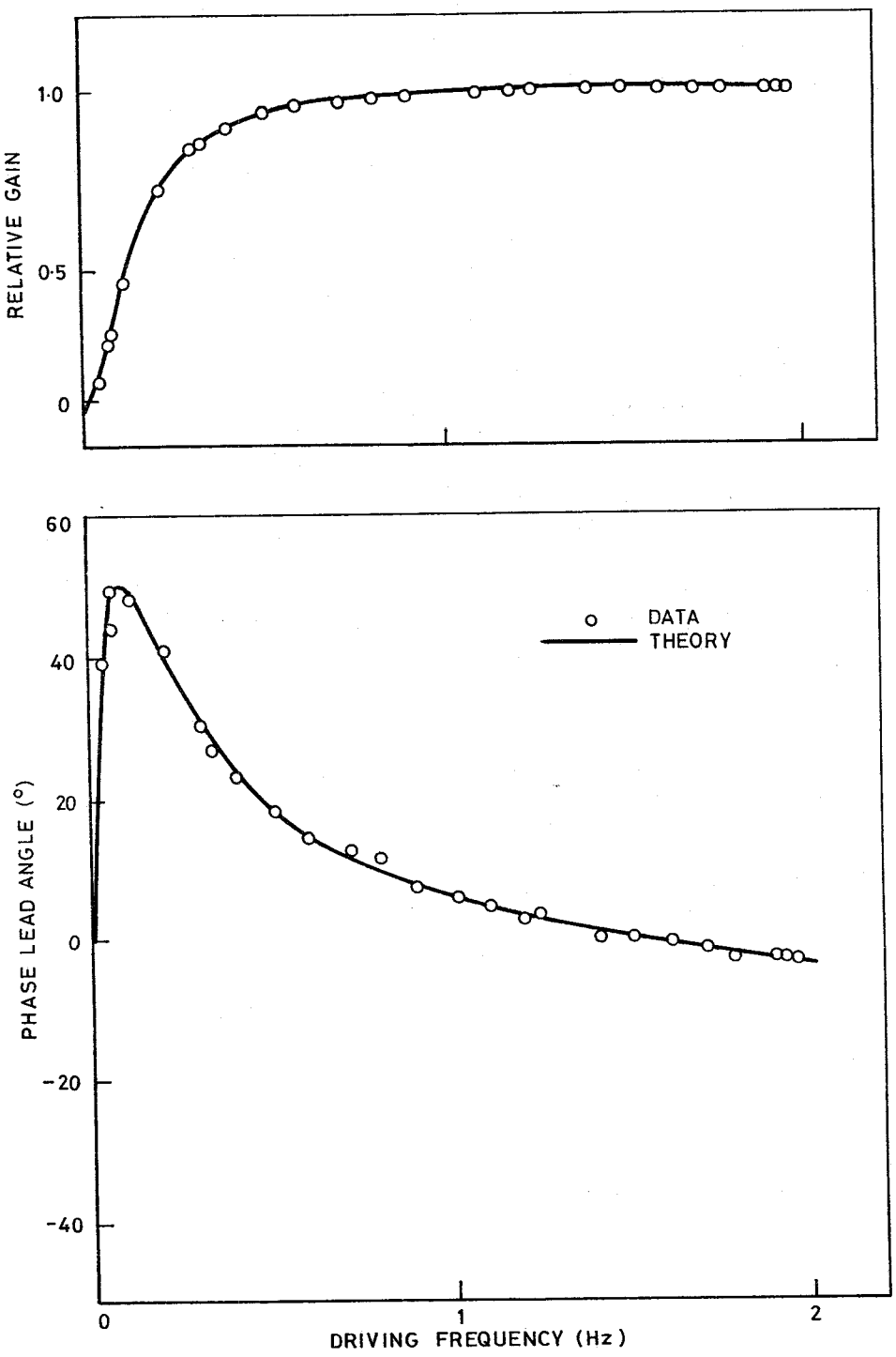

Figure 6. Pitch axis frequency response of the No. 3 gimbal system

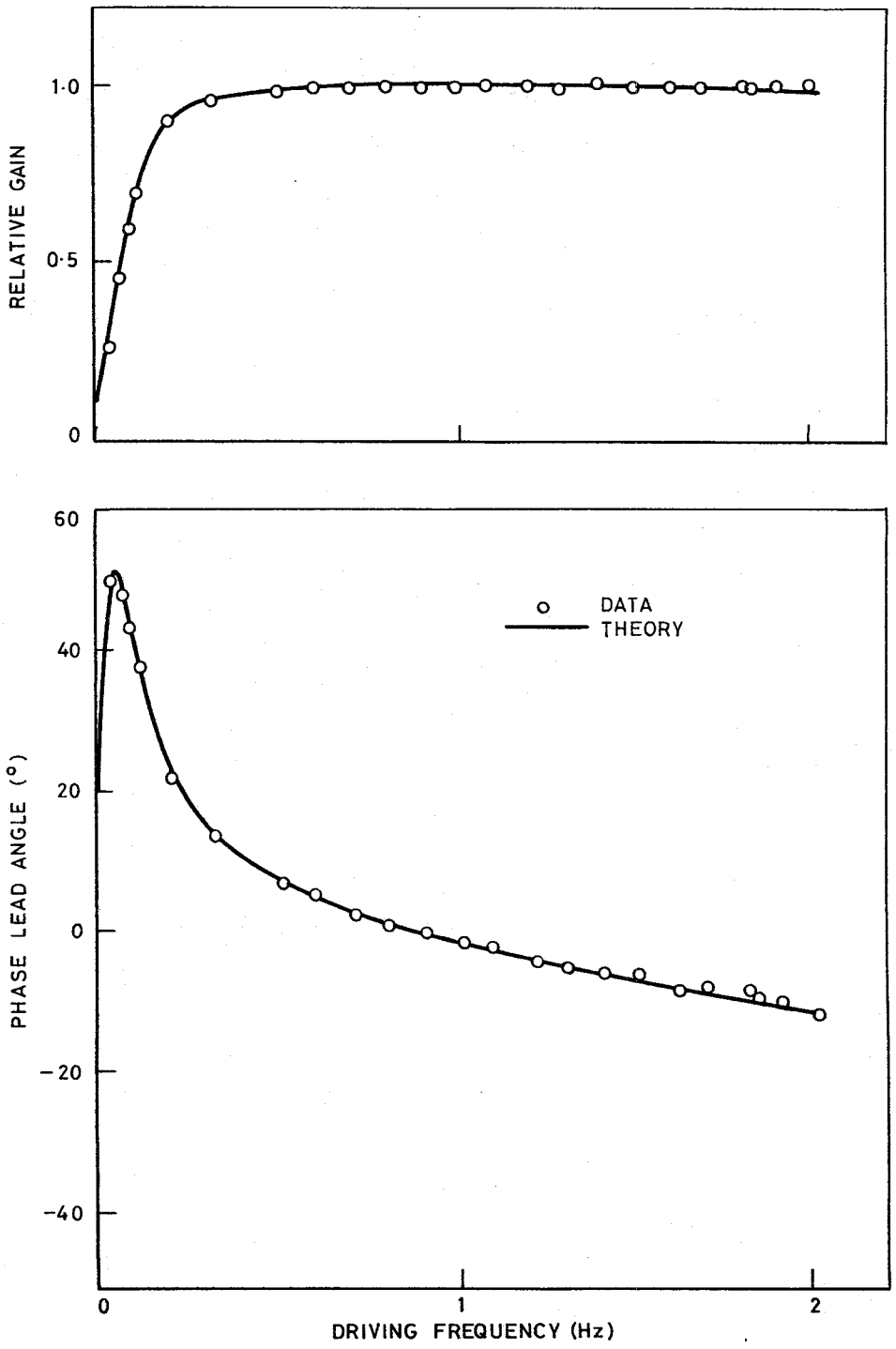

Figure 7. Roll axis frequency response of the No. 3 gimbal system

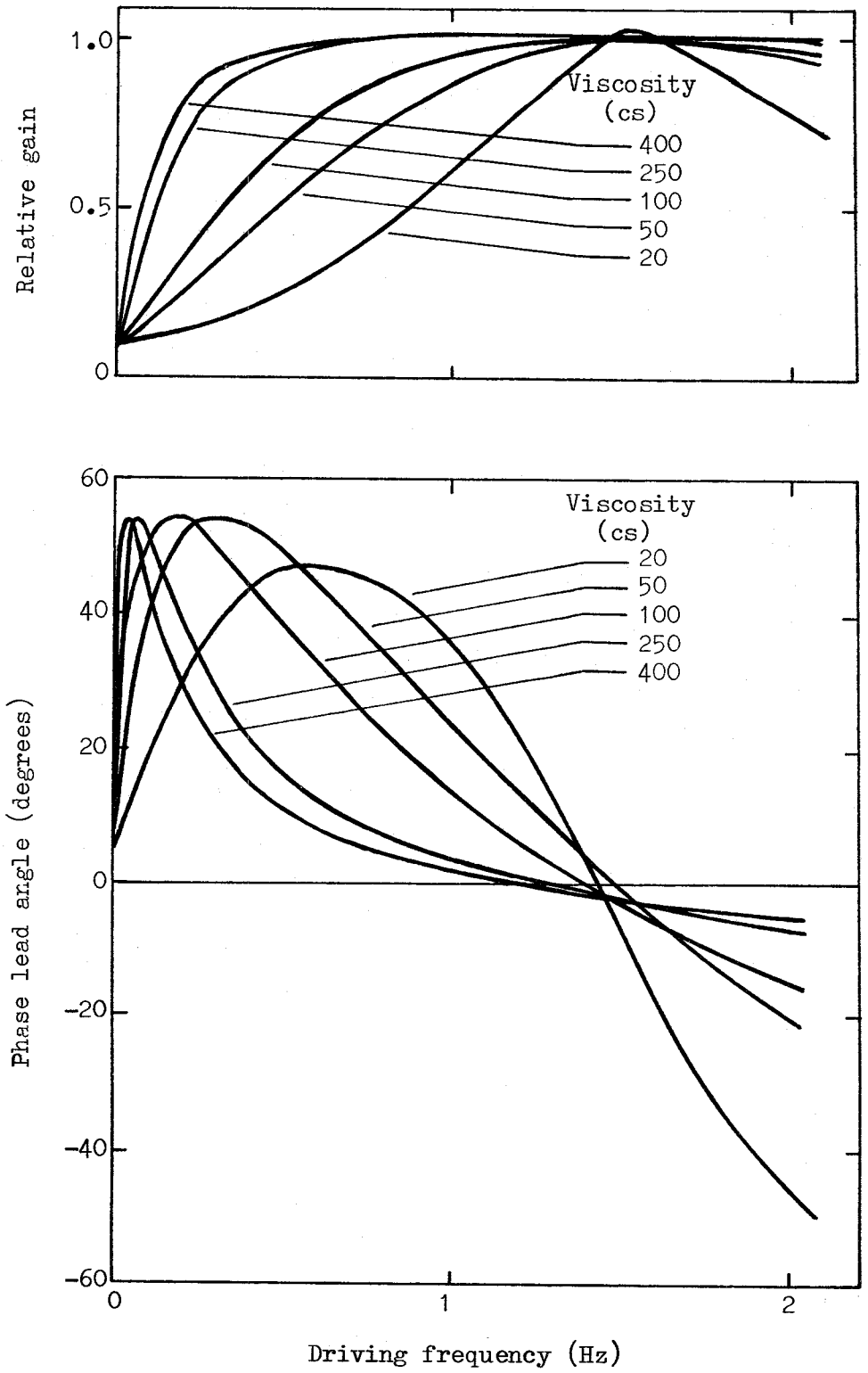

Figure 8. Fitted pitch axis frequency responses of the modified No. 3 gimbal system

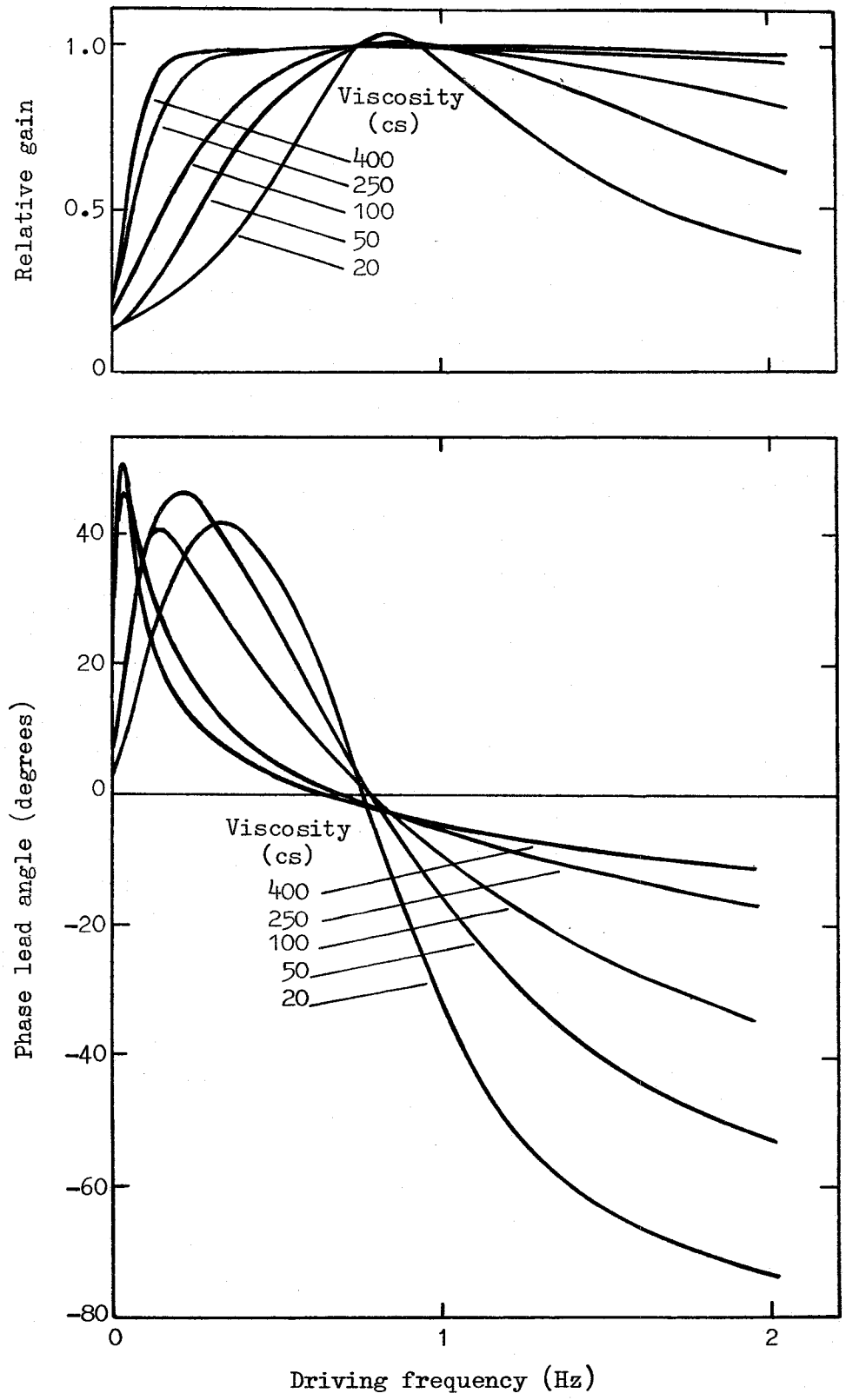

Figure 9. Fitted roll axis frequency responses of the modified No. 3 gimbal system

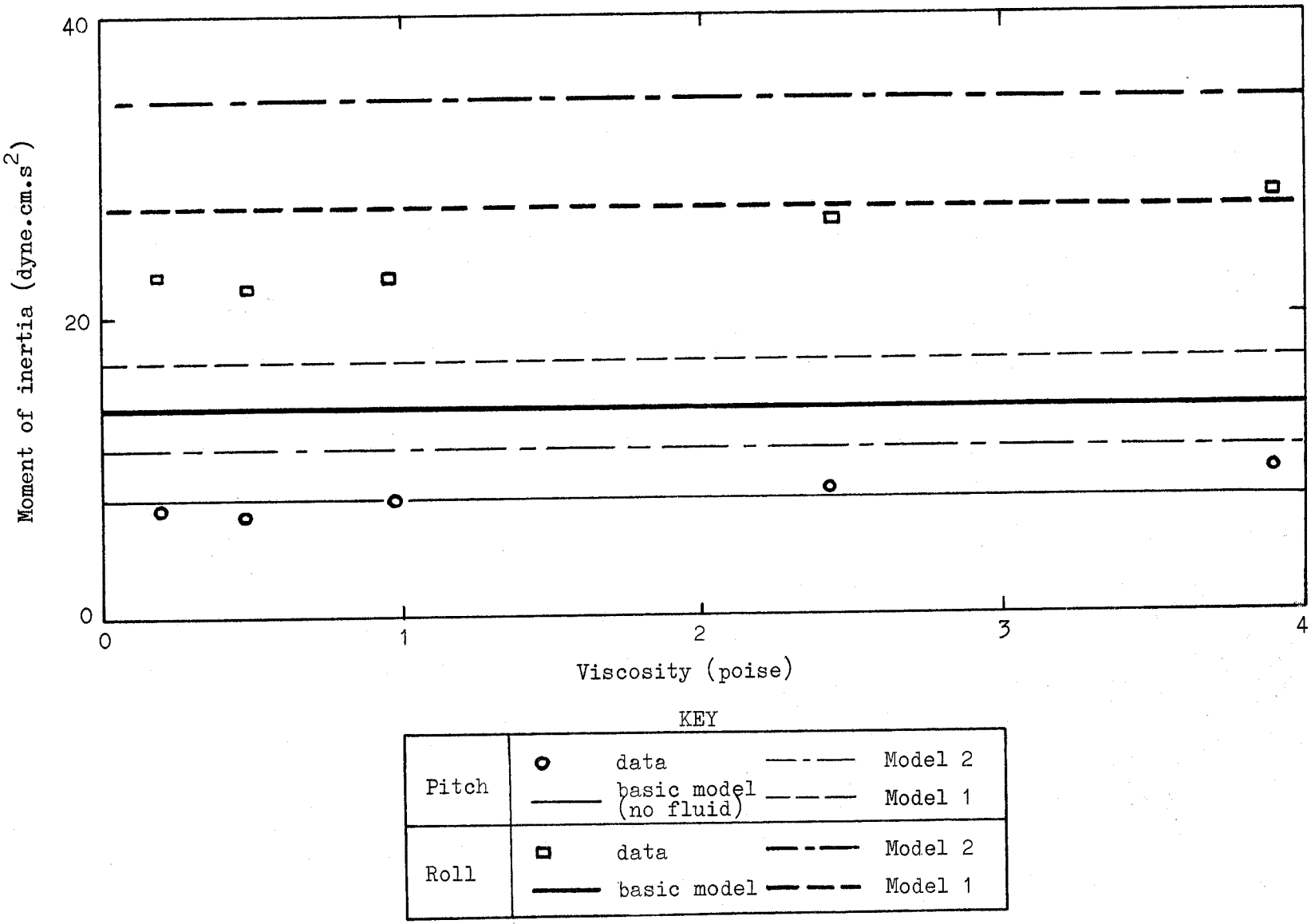

Figure 10. Moments of inertia vs oil viscosity

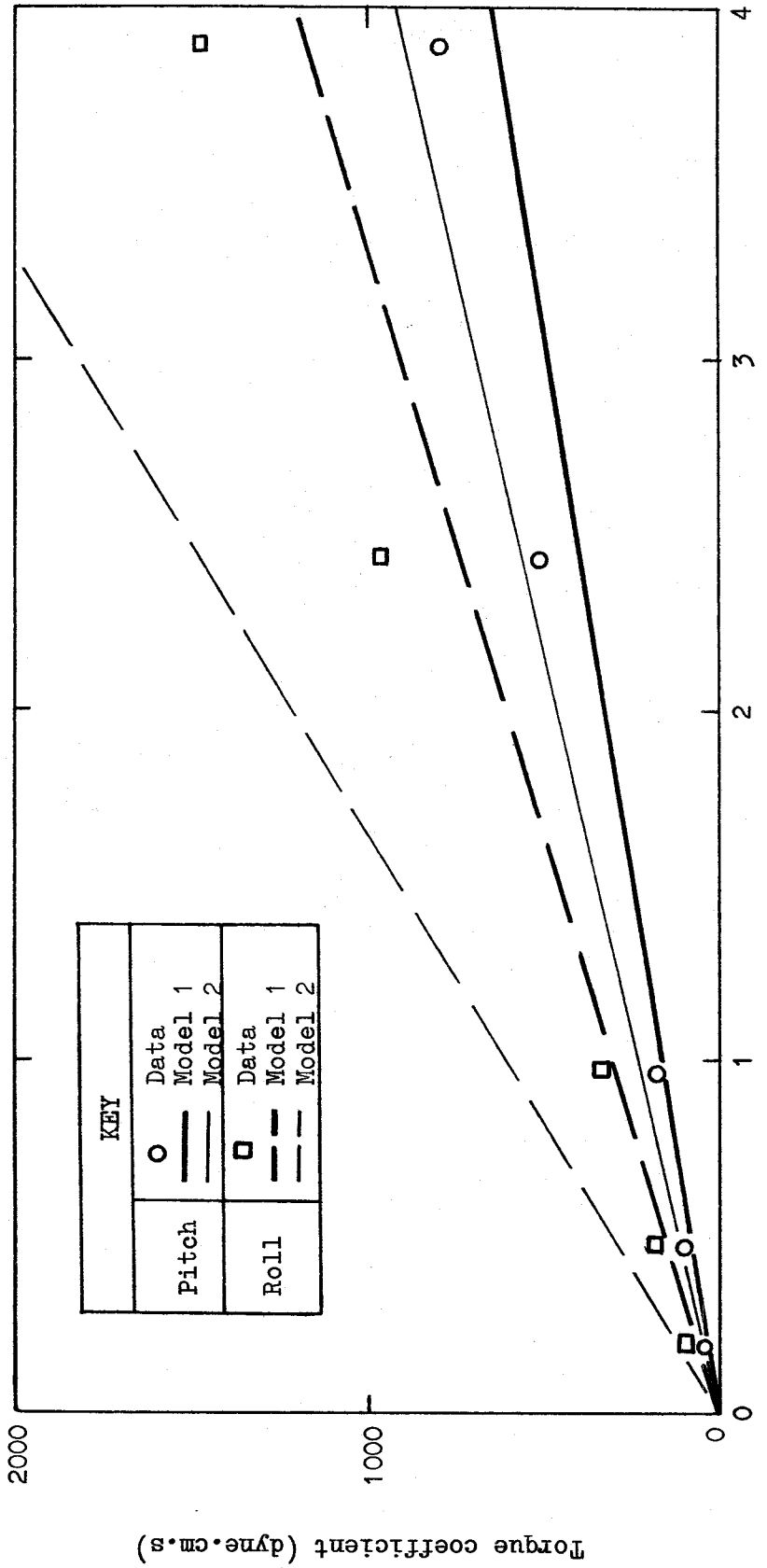

Figure 11. Viscous torgue coefficients vs oil viscosity

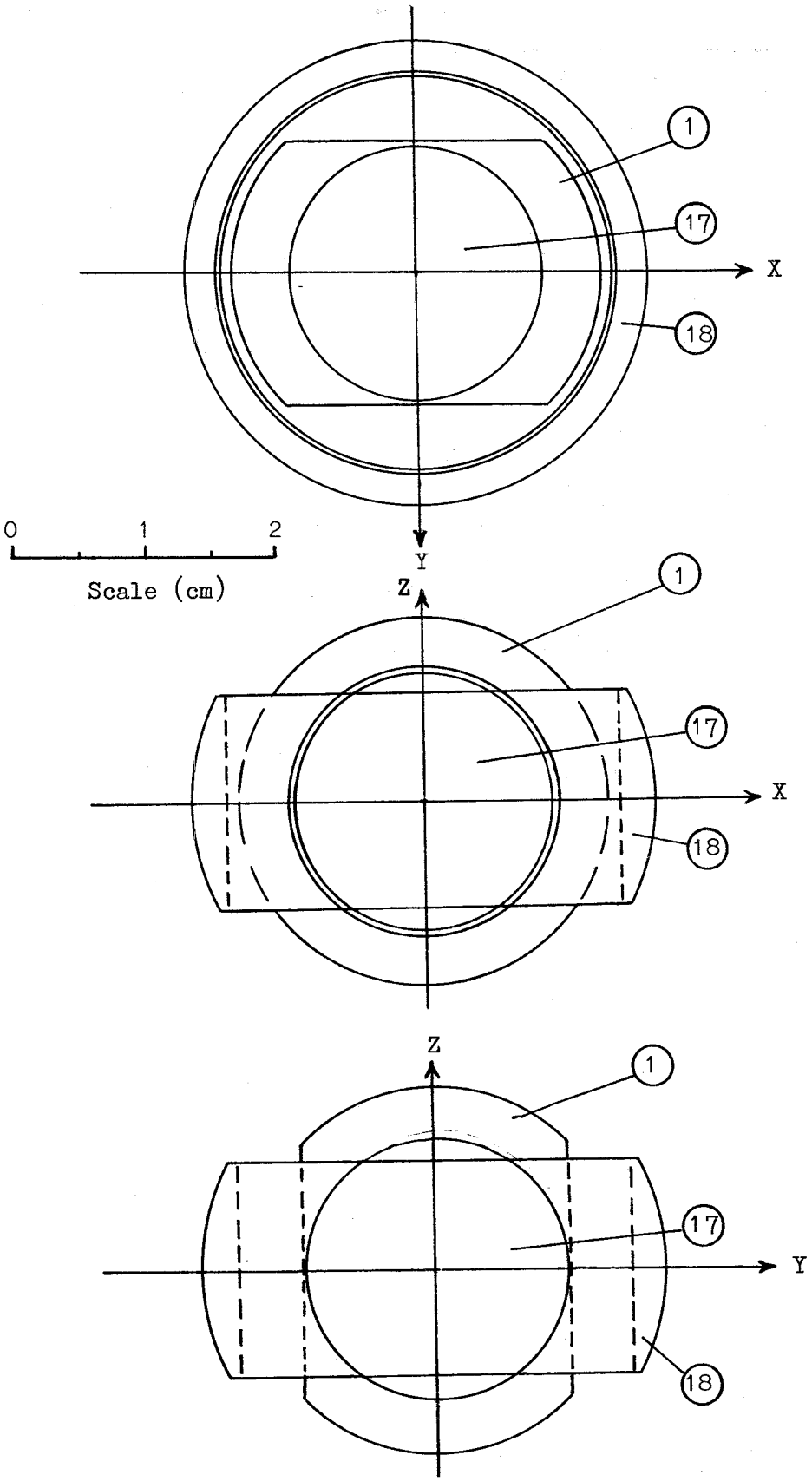

Figure 12. Model geometry for computation of moments of inertia (gimbal ring, skin and internal sphere components)

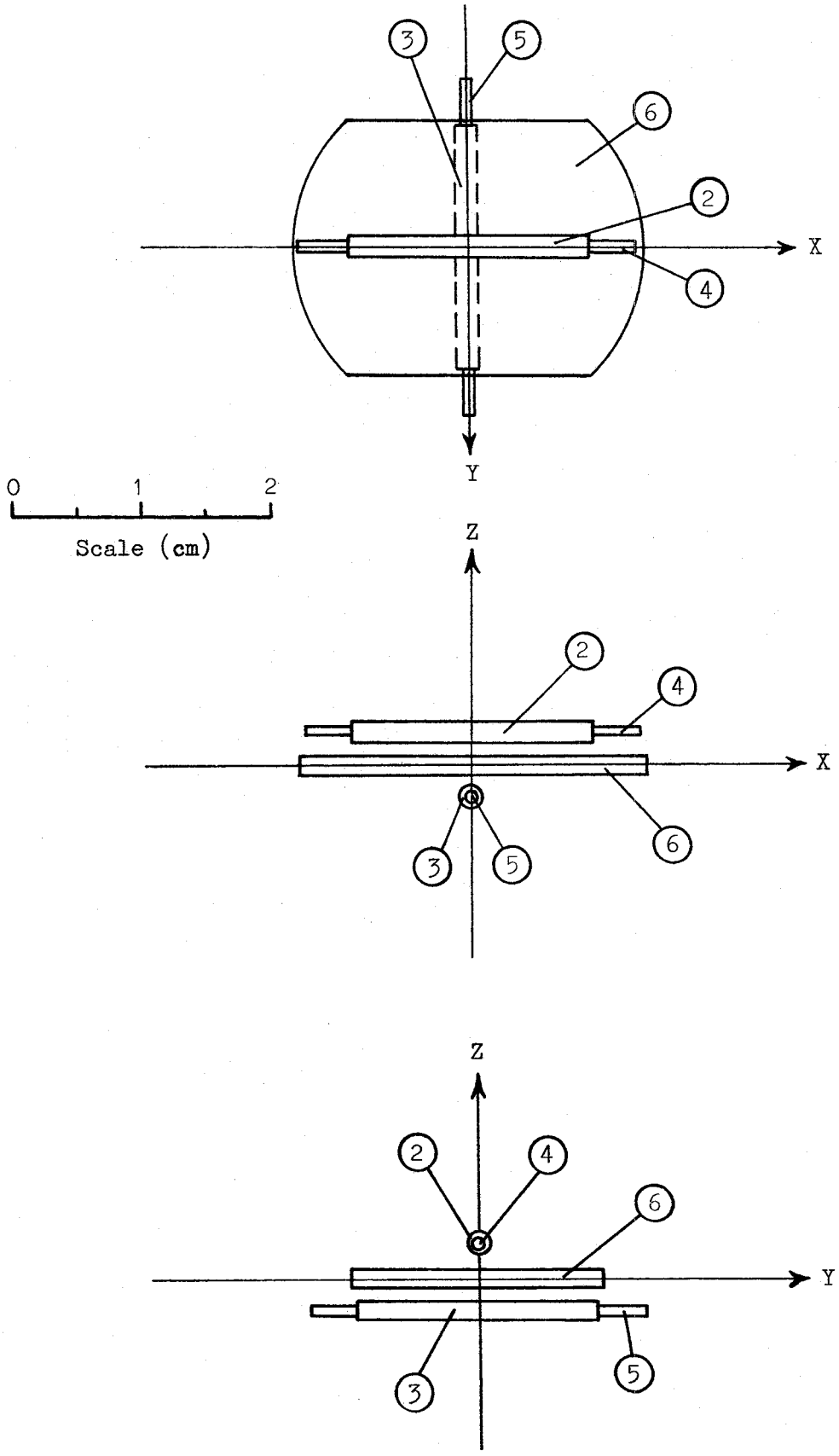

Figure 13. Model geometry for computation of moments of inertia (magnetometer and base plate components)

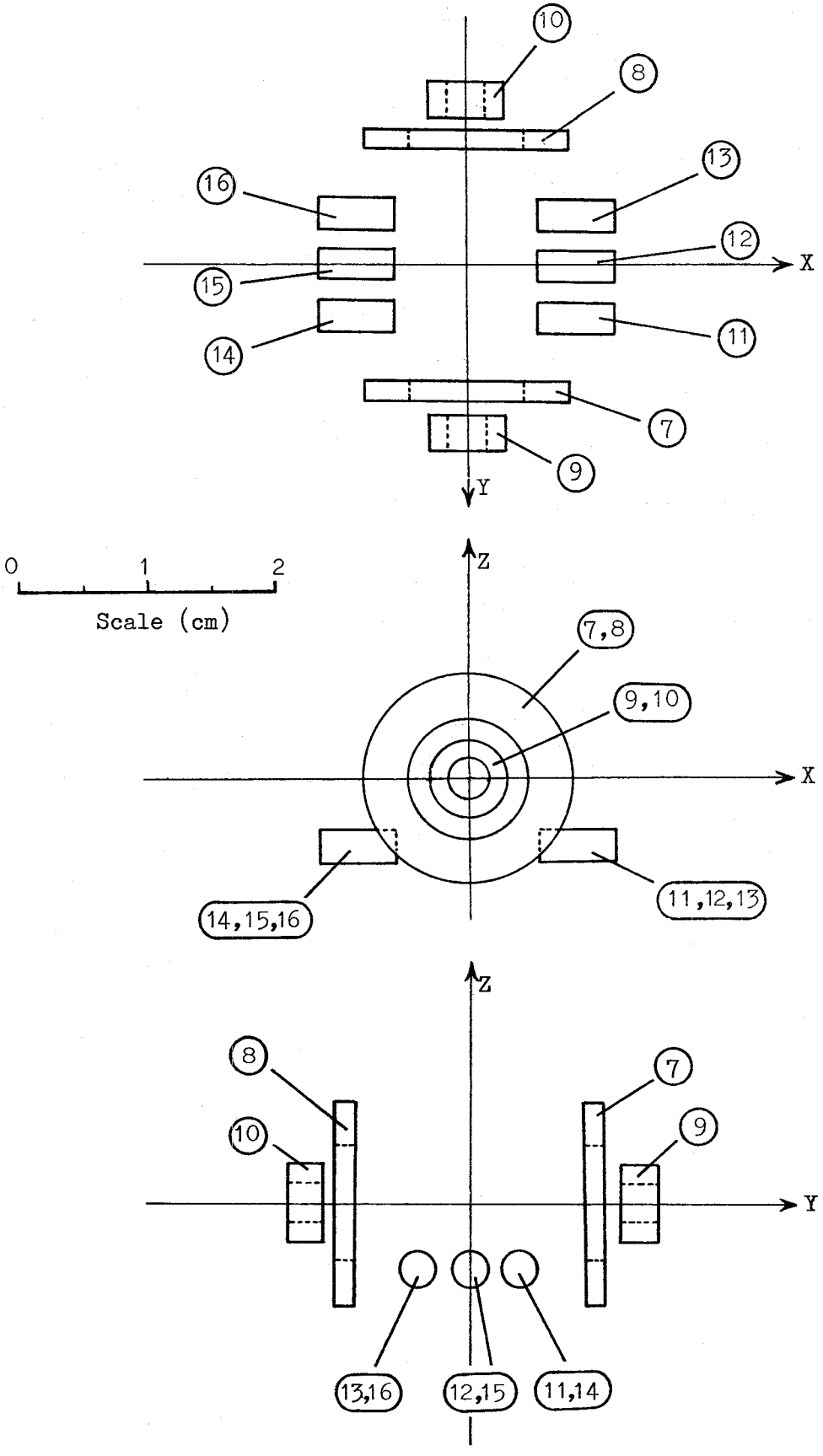

Figure 14. Model geometry for computation of moments of inertia (disc, bush and screw components)

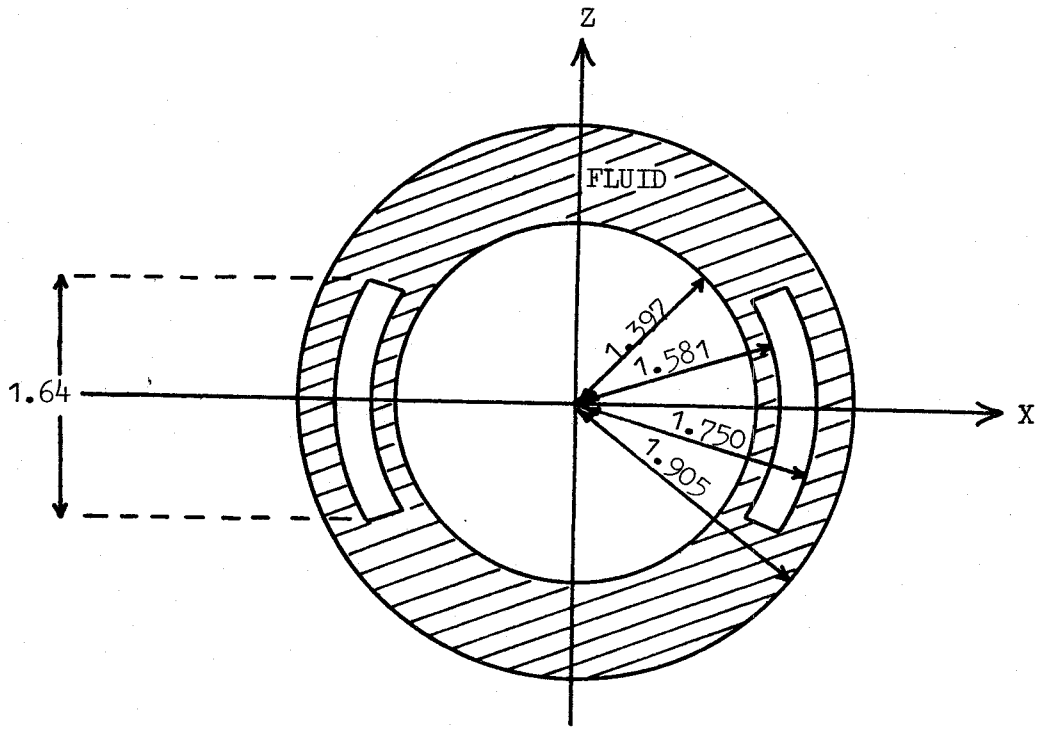

(vertical section on any diameter)

Figure 15. Model geometry of the gimbal system for computation of viscous torque coefficients, and moments of inertia of fluid

DOCUMENT CONTROL DATA SHEET

Security classification of this page: UNCLASSIFIED

1 DOCUMENT NUMBERS

AR Number: AR-001-399

Report Number: ERL-0037-TR

Other Numbers:

2 SECURITY CLASSIFICATION

a. Complete Document: Unclassified

b. Title in Isolation: Unclassified

c. Summary in Isolation: Unclassified

3 TITLE: THE FREQUENCY RESPONSE OF A PARTICULAR GIMBAL SYSTEM TO COHERENT ROTATION AND ACCELERATION EXCITATION

4 PERSONAL AUTHOR(S):

R.F. Dancer

5 DOCUMENT DATE: December 1978

6 6.1 TOTAL NUMBER OF PAGES: 61

6.2 NUMBER OF REFERENCES: 2

7 7.1 CORPORATE AUTHOR(S):

Electronics Research Laboratory

7.2 DOCUMENT SERIES AND NUMBER

Electronics Research Laboratory 0037-TR

8 REFERENCE NUMBERS

a. Task:

b. Sponsoring Agency:

9 COST CODE:

10 IMPRINT (Publishing organisation)

Defence Research Centre Salisbury

11 COMPUTER PROGRAM(S) (Title(s) and language(s))

12 RELEASE LIMITATIONS (of the document):

Approved for public release

12.0	OVERSEAS	NO		P.R.	1	A		B		C		D		E	

Security classification of this page: UNCLASSIFIED

Security classification of this page: Unclassified

13 ANNOUNCEMENT LIMITATIONS (of the information on these pages):

No limitation

14 DESCRIPTORS:

a. EJC Thesaurus Terms

Gimbals
Frequency response
Moments of inertia
Pivots
Iapis gimbal system

b. Non-Thesaurus Terms

15 COSATI CODES:

1707

16 LIBRARY LOCATION CODES (for libraries listed in the distribution):

AACA SD SR SW NL

17 SUMMARY OR ABSTRACT:
(if this is security classified, the announcement of this report will be similarly classified)

The general theoretical expression for the frequency response of a gimbal system to a joint rotation/acceleration driving force is derived. Theoretical estimates of physical system parameters are made for a particular gimbal system. Experimental verification of these theories is obtained by measurements of the rotationally excited response of the gimbal system.

Security classification of this page: UNCLASSIFIED